



RESEARCH PAPER

# Shade compromises the photosynthetic efficiency of NADP-ME less than that of PEP-CK and NAD-ME C<sub>4</sub> grasses

Balasaheb V. Sonawane<sup>1,2,\*</sup>, Robert E. Sharwood<sup>3</sup>, Spencer Whitney<sup>3</sup> and Oula Ghannoum<sup>1</sup>

<sup>1</sup> ARC Centre of Excellence for Translational Photosynthesis and Hawkesbury Institute for the Environment, Western Sydney University, NSW 2753, Australia

<sup>2</sup> School of Biological Sciences, Washington State University, Pullman, WA 99164, USA

<sup>3</sup> ARC Centre of Excellence for Translational Photosynthesis and Research School of Biology, Australian National University, Canberra, ACT 2601, Australia

\* Correspondence: [b.sonawane@wsu.edu](mailto:b.sonawane@wsu.edu)

Received 17 December 2017; Editorial decision 19 March 2018; Accepted 19 March 2018

Editor: Christine Raines, University of Essex, UK.

## Abstract

The high energy cost and apparently low plasticity of C<sub>4</sub> photosynthesis compared with C<sub>3</sub> photosynthesis may limit the productivity and distribution of C<sub>4</sub> plants in low light (LL) environments. C<sub>4</sub> photosynthesis evolved numerous times, but it remains unclear how different biochemical subtypes perform under LL. We grew eight C<sub>4</sub> grasses belonging to three biochemical subtypes [NADP-malic enzyme (NADP-ME), NAD-malic enzyme (NAD-ME), and phosphoenolpyruvate carboxykinase (PEP-CK)] under shade (16% sunlight) or control (full sunlight) conditions and measured their photosynthetic characteristics at both low and high light. We show for the first time that LL (during measurement or growth) compromised the CO<sub>2</sub>-concentrating mechanism (CCM) to a greater extent in NAD-ME than in PEP-CK or NADP-ME C<sub>4</sub> grasses by virtue of a greater increase in carbon isotope discrimination ( $\Delta_P$ ) and bundle sheath CO<sub>2</sub> leakiness ( $\phi$ ), and a greater reduction in photosynthetic quantum yield ( $\Phi_{max}$ ). These responses were partly explained by changes in the ratios of phosphoenolpyruvate carboxylase (PEPC)/initial Rubisco activity and dark respiration/photosynthesis ( $R_d/A$ ). Shade induced a greater photosynthetic acclimation in NAD-ME than in NADP-ME and PEP-CK species due to a greater Rubisco deactivation. Shade also reduced plant dry mass to a greater extent in NAD-ME and PEP-CK relative to NADP-ME grasses. In conclusion, LL compromised the co-ordination of the C<sub>4</sub> and C<sub>3</sub> cycles and, hence, the efficiency of the CCM to a greater extent in NAD-ME than in PEP-CK species, while CCM efficiency was less impacted by LL in NADP-ME species. Consequently, NADP-ME species are more efficient at LL, which could explain their agronomic and ecological dominance relative to other C<sub>4</sub> grasses.

**Keywords:** Biochemical subtypes, C<sub>4</sub> photosynthesis, CO<sub>2</sub>-concentrating mechanism, low light, shade.

## Introduction

C<sub>4</sub> photosynthesis is characterized by the operation of a CO<sub>2</sub>-concentrating mechanism (CCM) whereby atmospheric CO<sub>2</sub> is initially fixed in the mesophyll cells (MCs) into C<sub>4</sub> acids. These acids are subsequently decarboxylated in the bundle

sheath cells (BSCs) releasing CO<sub>2</sub> where Rubisco, the ultimate CO<sub>2</sub>-fixing enzyme, is located (Hatch, 1987). The CCM serves to raise the CO<sub>2</sub> concentration in the BSCs, thus curbing photorespiration and CO<sub>2</sub>-saturating photosynthesis at

current ambient CO<sub>2</sub> concentrations ([CO<sub>2</sub>]) under high light (Hatch, 1987; Kanai and Edwards, 1999). The CCM requires additional energy costs compared with the C<sub>3</sub> cycle associated with the regeneration of the C<sub>3</sub> precursor phosphoenolpyruvate (PEP) and the overcycling of CO<sub>2</sub>. Nevertheless, under warm temperatures, C<sub>4</sub> plants have a superior photosynthetic quantum yield ( $\Phi_{\max}$ ) relative to C<sub>3</sub> plants (Ehleringer and Björkman, 1977; Pearcy *et al.*, 1981; Ehleringer and Pearcy, 1983; Zhu *et al.*, 2008). This explains the ecological dominance of C<sub>4</sub> plants in open, high light (HL) environments and their disproportionately high global productivity relative to their small taxonomic representation (Ehleringer *et al.*, 1997; Brown, 1999; Edwards *et al.*, 2010).

Despite their success under HL, C<sub>4</sub> plants experience low light (LL) under natural conditions. C<sub>4</sub> crops and grasses can form dense canopies where a significant proportion of the leaf area is shaded, in addition to short-term LL exposures during the course of the day (Sage, 2014; Ort *et al.*, 2015). Numerous C<sub>4</sub> grasses are adapted to the shade of the forest interior (Sage and Pearcy, 2000). Shading is expected to increase in the understorey of C<sub>4</sub> grass-dominated ecosystems with predicted woody thickening under increasing atmospheric [CO<sub>2</sub>] (Bond and Midgley, 2012; Saintilan and Rogers, 2015). Consequently, it is important to investigate the efficiency of C<sub>4</sub> photosynthesis under LL across diverse C<sub>4</sub> plants.

C<sub>4</sub> photosynthesis has evolved independently many times, resulting in three biochemical subtypes named after the primary C<sub>4</sub> acid decarboxylase enzyme found in the BSCs, and they are NADP-malic enzyme (ME), NAD-ME, and phosphoenolpyruvate carboxykinase (PEP-CK) (Hatch 1987). PEP-CK operates as a secondary decarboxylase in many C<sub>4</sub> species (Leegood and Walker, 2003; Furbank, 2011; Sharwood *et al.*, 2014; Wang *et al.*, 2014). However, the primary decarboxylase is generally associated with a suite of anatomical, biochemical, and physiological features (Gutierrez *et al.*, 1974; Hattersley, 1992; Kanai and Edwards, 1999; Ghannoum *et al.*, 2011), making it a suitable classification basis for the purpose of the current study investigating the efficiency of the C<sub>4</sub>-CCM. The grass family includes species from all biochemical subtypes (Sage and Pearcy, 2000; Edwards *et al.*, 2010), but our understanding of how different C<sub>4</sub> subtypes respond and acclimate to LL environments remains limited.

It is well demonstrated that the C<sub>4</sub> subtypes have different leaf dry matter carbon isotope composition ( $\delta^{13}\text{C}$ ) and  $\Phi_{\max}$ . In particular, C<sub>4</sub> grasses with the NAD-ME subtype (i.e. NAD-ME as the primary decarboxylase) show lower leaf  $\delta^{13}\text{C}$  (i.e. more negative values which are closer to the C<sub>3</sub> range) and  $\Phi_{\max}$ , while NADP-ME and PEP-CK species (i.e. those with NADP-ME and PEP-CK as the primary decarboxylases, respectively) show the highest and intermediate values, respectively (Hattersley, 1982; Ehleringer and Pearcy, 1983). There is a paucity of data comparing the response to shade of leaf  $\delta^{13}\text{C}$  and  $\Phi_{\max}$  of the various C<sub>4</sub> subtypes. Using 14 C<sub>4</sub> grasses, Buchmann *et al.* (1996) found that leaf  $\delta^{13}\text{C}$  values of NAD-ME species were most impacted by shade, followed by PEP-CK and NADP-ME species. In a large survey of C<sub>4</sub> grasses, von Caemmerer *et al.* (2014) reported that leaf  $\delta^{13}\text{C}$  was equally affected by growing season irradiance

(winter versus summer) in NAD-ME and NADP-ME grasses. This discrepancy may be due to the fact that carbon isotope composition and discrimination are not significantly affected until photosynthetic photon flux density (PPFD) decreases below 700  $\mu\text{mol m}^{-2} \text{s}^{-1}$  (Buchmann *et al.*, 1996).

In C<sub>4</sub> plants, both photosynthetic and post-photosynthetic discrimination factors determine leaf  $\delta^{13}\text{C}$  (Farquhar, 1983; von Caemmerer *et al.*, 2014). Reduced leaf  $\delta^{13}\text{C}$  under LL may be attributed to increased photosynthetic carbon isotope discrimination ( $\Delta_P$ ) and BSC leakiness ( $\phi$ ) as a result of reduced CCM efficiency (Henderson *et al.*, 1992). For example, LL may reduce the activity of the C<sub>3</sub> cycle to a greater extent than that of the C<sub>4</sub> cycle, leading to greater overcycling. In turn, this will lead to higher  $\phi$  and energetic cost of operating the C<sub>4</sub>-CCM. Consequently, we hypothesized that LL will differentially compromise the C<sub>4</sub>-CCM efficiency depending on the biochemical subtype. In particular, we predicted that LL will increase leaf  $\delta^{13}\text{C}$  and  $\Delta_P$ , and reduce  $\Phi_{\max}$  to a greater extent in NAD-ME grasses, followed by PEP-CK and NADP-ME species (Hypothesis 1).

Short- and long-term photosynthetic responses to LL are expected to differ. Following long-term exposure to LL (shade), the photosynthetic apparatus commonly acclimates to maximize light use efficiency (Björkman, 1981; Boardman, 1977; Sage and McKown, 2006). Depending on the plant species and ecotype, acclimation may be minimal or profound (Ward and Woolhouse, 1986*a, b*; Björkman and Holmgren, 1966). Overall, acclimation of C<sub>3</sub> and C<sub>4</sub> plants to shade involves partitioning of photosynthetic nitrogen (N) away from Rubisco towards the light-harvesting processes (Boardman, 1977; Björkman, 1981; Hikosaka and Terashima, 1995; Evans and Poorter, 2001; Walters, 2005; Tazoe *et al.*, 2006; Pengelly *et al.*, 2010). NAD-ME species are known to have higher leaf N content and a greater N fraction invested in Rubisco relative to NADP-ME species (Ghannoum *et al.*, 2005). Hence, the former subtype may have a greater flexibility to reallocate N under shade especially since, as mentioned above, LL is expected to reduce the activity of the C<sub>3</sub> cycle (e.g. Rubisco) more than the C<sub>4</sub> cycle [e.g. phosphoenolpyruvate carboxylase (PEPC)]. However, optimal photosynthetic acclimation of C<sub>4</sub> photosynthesis to shade is expected to involve parallel reductions in the activities of the C<sub>3</sub> and C<sub>4</sub> cycles in order to curb leakiness and maintain an efficient CCM and quantum yield (Bellasio and Griffiths, 2014*a, b*), which does not seem to be the case for NAD-ME species in Buchmann *et al.* (1996). Consequently, we hypothesized that NAD-ME species will exhibit a greater photosynthetic acclimation in response to shade relative to the other two subtypes. This will manifest as a greater photosynthetic down-regulation and higher leakiness in the LL-acclimated leaves of NAD-ME species relative to the other two subtypes (Hypothesis 2).

To address these two hypotheses, we investigated the photosynthetic responses of eight C<sub>4</sub> grasses belonging to three biochemical subtypes (Table 1) to short-term (200  $\mu\text{mol}$  quanta  $\text{m}^{-2} \text{s}^{-1}$  versus 2000  $\mu\text{mol}$  quanta  $\text{m}^{-2} \text{s}^{-1}$ ) and long-term (16% versus 100% sunlight; *Supplementary Fig. S1A* at JXB online) light treatments. We sought to elucidate the underlying mechanisms by describing changes in photosynthetic rates and enzyme activities, and in the CCM efficiency

as described by leakiness and quantum yield. Our results indicated that NADP-ME species are generally more efficient at LL due to effective co-ordination of the C<sub>4</sub> and C<sub>3</sub> cycles.

## Materials and methods

### Plant culture

The experiment was conducted in a naturally lit glasshouse chamber (5 m<sup>3</sup>) during the Australian summer. Within the chamber, an aluminium structure (1.5 × 5 m<sup>3</sup>) was covered with white shade cloth (Premium Hortshade Light, Model No. 428976, Coolaroo, VIC, Australia). A PPFD of ~100 μmol quanta m<sup>-2</sup> s<sup>-1</sup> was achieved inside the shade structure by adjusting the number of cloth layers. The impact of heavy shade during cloudy days was minimized by supplementing external growth light (LimiGrow Pro S325, Emeryville, CA, USA) to achieve a leaf-level PPFD of 100 μmol m<sup>-2</sup> s<sup>-1</sup>. The chamber temperature was maintained at 28/22 °C for day/night with an in-built glasshouse temperature-controlled system. The air temperature and relative humidity (RH) at leaf level were monitored using Rotronic HC2-S3 (Bassersdorf, Switzerland) sensors placed in a shield vented with a 12 V fan. A Licor quantum sensor (LI-190, Lincoln, NE, USA) was mounted at the leaf level to monitor incident PPFD in the unshaded and shaded glasshouse structure. Data from these sensors were stored using a Licor data logger (LI-1400). Through the experiment, average midday ambient PPFD, T, and RH at leaf level were 741 μmol m<sup>-2</sup> s<sup>-1</sup>, 25 °C, and 69% in the sun treatment. These figures in the shade treatment were 119 μmol m<sup>-2</sup> s<sup>-1</sup>, 26 °C, and 65% (see [Supplementary Fig. S1C](#)). Hence, the shade treatment was equivalent to 16% of sunlight measured in the sun treatment, averaged over the experimental period ([Supplementary Fig. S1](#)). Instantaneous leaf temperature was measured using a hand-held, non-contact infrared thermometer (AGRI-THERM II™, Chino Hills, CA USA). On average, shaded leaves were 1–2 °C cooler than sun leaves ([Supplementary Fig. S1D](#)).

Locally collected soil was sun dried ([Pinto et al., 2014](#)), coarsely sieved, and added to 3.5 litre cylindrical pots. Pots were watered to 100% capacity and transferred to the glasshouse chamber. Seeds for grasses used in this study ([Table 1](#)) were obtained from the Australian Plant Genetic Resources Information System (QLD, Australia) and Queensland Agricultural Seeds Pty. Ltd. (Toowoomba, Australia). In the current study, we used 2–3 representative species belonging to each of the C<sub>4</sub> subtypes. Within each subtype, species were selected from different C<sub>4</sub> origins (tribes in [Table 1](#)) to randomize the C<sub>4</sub> origin effect, and hence focus on the subtype effect.

Seeds were germinated in a commercial Osmocote® professional, seed raising and cutting mix (Scotts, Bella Vista, NSW, Australia). Three to four weeks after germination, two healthy seedlings were transplanted into each of the soil-filled and pre-irrigated pots. A week later, one healthy seedling was left in each pot while the other was removed. Plants were allowed to grow until the 5–6 leaf stage in full sunlight before they were transferred to the shade treatment. There were eight pots per species and light treatment. Pots

were randomly positioned and regularly rotated within each treatment throughout the experiment. Plants were well watered daily with added commercial soluble fertilizer (Aquasol, N:P:K=23.3:3.95:14; Yates, Wetherill Park, NSW, Australia).

### Leaf gas exchange measurements

Leaf gas exchange was measured with a portable open gas exchange system (LI-6400XT, LI-COR). The youngest last fully expanded leaf (LFEL) on the main stem of a 6- to 9-week-old plant was measured at a leaf temperature of 28 °C between 10.00 h and 14.00 h. Shaded plants developed a minimum of three new leaves under shade before gas exchange measurements were made.

Each leaf was allowed to reach a steady state, at least 20 min, CO<sub>2</sub> assimilation rate (A) at ambient [CO<sub>2</sub>] of 407 μbar, PPFD of 2000 μmol m<sup>-2</sup> s<sup>-1</sup>, and RH of 50–70%. After this, a steady-state measurement [performed concurrently with tunable diode-laser (TDL) analysis; see below for details] was taken. Subsequently, the response of A to step increases of intercellular CO<sub>2</sub> (C<sub>i</sub>), the A–C<sub>i</sub> curve, was measured by raising the LI-6400XT leaf chamber [CO<sub>2</sub>] in 10 steps between 50 μbar and 1500 μbar. After completing the A–C<sub>i</sub> curve at PPFD 2000 μmol m<sup>-2</sup> s<sup>-1</sup>, the leaf was allowed to reach a steady state of gas exchange at saturating CO<sub>2</sub> (660 μbar) before measuring the responses to PPFD. The light response curve was measured from HL to LL (11 steps) followed by measurements of dark respiration (R<sub>d</sub>) at ambient [CO<sub>2</sub>] of 407 μbar after 20 min in a dark leaf chamber. Prior to LL steady-state measurement (performed concurrently with TDL analysis; see below for details), the same leaf was allowed to reach a steady-state A similarly to HL measurements, except PPFD was controlled at 250 μmol m<sup>-2</sup> s<sup>-1</sup>. This was followed by measuring the A–C<sub>i</sub> curve at the same light (LL) as described above. There were 3–4 replicates per treatment. The initial slope (IS) of the A–C<sub>i</sub> curve was estimated for the linear part of the A–C<sub>i</sub> curve measured at HL where C<sub>i</sub> is <55 μbar. The maximum CO<sub>2</sub> assimilation rate (A) on the A–C<sub>i</sub> curve was considered as the CO<sub>2</sub>-saturated rate (CSR). The A–C<sub>i</sub> curves measured at LL could not be used for accurate IS determination due to low overall rates. The light response curves were fitted using the following equation ([Ögren and Evans, 1993](#)):

$$A = \frac{(\Phi_{nls} \cdot I + A_{max}) - \sqrt{(\Phi_{nls} \cdot I + A_{max})^2 - 4 \cdot \theta \cdot I \cdot A_{max}}}{2 \cdot \theta} \quad (1)$$

where, I=absorbed irradiance, we assumed absorptance=0.85; A=CO<sub>2</sub> assimilation rate at given light; Φ<sub>nls</sub>=maximum quantum yield of PSII; A<sub>max</sub>=light-saturated CO<sub>2</sub> assimilation rate; and θ=curvature factor of the light response curve. In addition, the slope of a linear part of the light response curve (PPFD <120 μmol m<sup>-2</sup> s<sup>-1</sup>) was estimated as the ‘apparent’ maximum quantum yield of PSII (Φ<sub>max</sub>). We consider this estimate in our further analysis.

### Photosynthetic carbon isotope discrimination

Bundle sheath leakiness (φ) was determined by measuring real-time <sup>13</sup>CO<sub>2</sub>/<sup>12</sup>CO<sub>2</sub> isotope discrimination using a LI-6400XT interfaced with a tunable diode laser, TDL (TGA100, Campbell Scientific, Inc., Logan, UT, USA). The mean SD for repeated TDL measurements of δ<sup>13</sup>C values for a reference gas was 0.09‰. Observed photosynthetic carbon isotope discrimination against (Δ<sub>p</sub>) was calculated using ([Evans et al., 1986](#)):

$$\Delta_p = \frac{\xi \cdot (\delta_o - \delta_e)}{1 + \delta_o - \xi \cdot (\delta_o - \delta_e)} \quad (2)$$

$$\xi = \frac{C_e}{C_e - C_o} \quad (3)$$

**Table 1.** List of C<sub>4</sub> grasses used in the current study

C <sub>4</sub> subtype	C <sub>4</sub> tribe	Species
NADP-ME	Paniceae	<i>Cenchrus ciliaris</i> <i>Panicum antidotale</i>
	Andropogoneae	<i>Sorghum bicolor</i> <i>Zea mays</i>
PEP-CK	Paniceae	<i>Megathyrsus maximus</i>
	Chloridoideae	<i>Chloris gayana</i>
NAD-ME	Paniceae	<i>Panicum coloratum</i>
	Chloridoideae	<i>Leptochloa fusca</i>

where  $\delta_e$ ,  $\delta_o$ ,  $C_e$ , and  $C_o$  are the  $\delta^{13}\text{C}$  ( $\delta$ ) and  $\text{CO}_2$  mole fraction ( $C$ ) of the air entering (e) and leaving (o) the leaf chamber measured with the TDL-LI-6400 set up. Leakiness at high light ( $\phi_h$ ) was calculated using the model of Farquhar (1983) as modified by Pengelly *et al.* (2010, 2012) and von Caemmerer *et al.* (2014):

$$\phi_h = \frac{\left(\frac{1-t}{1+t}\right) \cdot \Delta_p - \frac{a'}{1+t} - (a_i - b'_4) \cdot \frac{A}{g_m \cdot C_a} - \left(b'_4 - \frac{a'}{1+t}\right) \cdot \frac{C_i}{C_a}}{(b'_3 - s) \cdot \left(\frac{C_i}{C_a} - \frac{A}{C_a \cdot g_m}\right)} \quad (4)$$

where  $t$ , the ternary correction factor, is calculated as per Farquhar and Cernusak (2012):

$$t = \frac{(1+a') \cdot E}{2 \cdot g'_{ac}}, \quad (5)$$

where  $E$  is the transpiration rate,  $g'_{ac}$  the total conductance to  $\text{CO}_2$  diffusion including boundary layer and stomatal conductance (von Caemmerer and Farquhar, 1981). The combined fractionation factor through the leaf boundary layer and stomata is denoted by  $a'$ ,

$$a' = \frac{a_b \cdot (C_a - C_{ls}) + a \cdot (C_{ls} - C_i)}{C_a - C_i} \quad (6)$$

Definition and units for the variables included in the above equation are described in Table 2, but briefly,  $C_a$ ,  $C_i$ , and  $C_{ls}$  are the ambient, intercellular and leaf surface  $\text{CO}_2$  mole fractions, respectively;  $a_b$  (2.9‰) is the fractionation occurring through diffusion in the boundary layer;  $s$  (1.8‰) is the fractionation during leakage of  $\text{CO}_2$  out of the bundle sheath assuming there is no  $\text{HCO}_3^-$  leakage out of BSCs (Henderson *et al.*, 1992);  $a$  (4.4‰) is the fractionation due to diffusion in air (Evans *et al.*, 1986); and  $a_i$  is the fractionation factor associated with the dissolution of  $\text{CO}_2$  and diffusion through water (1.8‰).

$b'_3$  and  $b'_4$  are defined as in von Caemmerer *et al.* (2014):

$$b'_3 = b_3 - e \cdot \left( \frac{R_d}{A + R_d} - \frac{0.5 \cdot R_d}{A + 0.5 \cdot R_d} \right) - f \cdot \frac{0.5 \cdot V_o}{V_c}, \quad (7)$$

and

$$b'_4 = b_4 - e \cdot \frac{0.5 \cdot R_d}{(A + 0.5 \cdot R_d)} \quad (8)$$

where  $b_3$  is the fractionation by Rubisco (30‰);  $b_4$  is the combined fractionation of the conversion of  $\text{CO}_2$  to  $\text{HCO}_3^-$  and PEP carboxylation (−5.41‰ at 28 °C) (Henderson *et al.*, 1992; Mook *et al.*, 1974);  $f$  is the fraction associated with photorespiration; and  $V_o$  and  $V_c$  are the rates of oxygenation and carboxylation, respectively. Under

HL we assumed no photorespiration, hence the term  $f \cdot \frac{0.5 \cdot V_o}{V_c} = 0$

(Pengelly *et al.*, 2010, 2012; Ubierna *et al.*, 2013; von Caemmerer *et al.*, 2014). The reference gas supplied to the LI-6400XT during gas exchange measurements had  $\delta^{13}\text{C} = -5.5\text{‰}$ . Therefore, the value for the fractionation factor  $e$  associated with respiration was calculated assuming recent photoassimilates as the respiratory substrate (Stutz *et al.*, 2014). Thus,  $e$  equalled the difference between  $\delta^{13}\text{C}$  in the  $\text{CO}_2$  sample line in LI-6400XT and that in the glasshouse chamber (−8‰; Tazoe *et al.* (2008)).  $A$  and  $R_d$  (von Caemmerer *et al.*, 2014) denote the  $\text{CO}_2$  assimilation rate and day respiration, respectively;  $R_d$  was assumed to equal measured dark respiration. We assumed mesophyll conductance,  $g_m = 1.4 \text{ mol m}^{-2} \text{ s}^{-1}$  at 28 °C (for  $\text{C}_4$  the model plant *Setaria viridis*) (Ubierna *et al.*, 2017).

Leakiness at low light ( $\phi_l$ ) was calculated as described by Bellasio and Griffiths (2014b) and Ubierna *et al.* (2013). Briefly, electron

transport flux ( $J_t$ ) at low light was derived by deploying the light-limited  $\text{C}_4$  photosynthesis model to calculate  $C_s$  ( $\text{CO}_2$  mole fraction in the bundle sheath),  $V_p$  (PEP carboxylation rate),  $V_c$  (Rubisco carboxylation rate), and  $V_o$  (Rubisco oxygenation rate) at LL using the  $\text{C}_4$  model (von Caemmerer, 2000) (see Supplementary Appendix S1). It should be noted that we used measured values for the fraction of PSII in BSCs,  $\alpha$  (0 for NADP-ME and 0.2 for PEP-CK and NAD-ME) and half of the reciprocal of Rubisco specificity,  $\gamma^*$  (0.000255, 0.00023, and 0.000233 for NADP-ME, NAD-ME, and PEP-CK, respectively) (Table 2; Sharwood *et al.*, 2016a) for biochemical subtypes of  $\text{C}_4$  photosynthesis during the calculation of  $J_t$ . These parameters were then used to calculate  $\bar{b}_4$  (the combined effects of fractionations by the  $\text{CO}_2$  dissolution, hydration, and PEPC activity at LL) and  $\bar{b}_3$  (Rubisco fractionation at LL by accounting for the fraction during respiration and photorespiration) (Farquhar, 1983; Ubierna *et al.*, 2013) to calculate  $\phi_l$  in the following equation,

$$\phi_l = \frac{\Delta_p \cdot (1-t) \cdot C_a - a' \cdot (C_a - C_i)}{\left( \frac{C_{bs} - C_m}{C_m} \right) \cdot \frac{-a_i \cdot (C_i - C_m) \cdot (1+t) - (1+t) \cdot C_m \cdot \bar{b}_4}{(1+t) \cdot [\bar{b}_3 \cdot C_{bs} - s \cdot (C_{bs} - C_m) + a_i \cdot (C_i - C_m)]} + a' \cdot (C_a - C_i) - C_a \cdot \Delta_p \cdot (1-t)} \quad (9)$$

other variables and unit are as defined in Table 2, but briefly  $C_m$  is the mesophyll  $\text{CO}_2$  mole fraction given by

$$C_m = C_i - \frac{A}{g_m} \quad (10)$$

Subtype-specific values for  $\alpha$  and  $\gamma^*$  improved the estimations of  $\phi_l$  as demonstrated in Supplementary Fig. S7.

#### Activity of Rubisco, PEPC, NADP-ME, NAD-ME, and PCK

Following gas exchange measurements, replicate discs (0.4–1 cm<sup>2</sup>) were rapidly frozen in liquid N then stored at −80 °C until analysed. Two sets of extractions were performed to complete the biochemical analysis. For Rubisco activity, activation, and content, PEPC and NADP-ME activity, and soluble protein assays, the extraction buffer was purged of  $\text{CO}_2$  overnight by bubbling a weak jet of nitrogen gas through the basic buffer [50 mM EPPS-NaOH (pH 7.8), 5 mM MgCl<sub>2</sub>, 1 mM EDTA]. Each leaf disc was extracted in 0.8 ml of ice-cold extraction buffer [50 mM EPPS-NaOH (pH 7.8), 5 mM DTT, 5 mM MgCl<sub>2</sub>, 1 mM EDTA, 10 µl of protease inhibitor cocktail (Sigma), 1% (w/v) polyvinyl polypyrrolidone (PVPP)] using a 2 ml Tenbroeck glass homogenizer kept on ice. Chlorophyll content was estimated according to Porra *et al.* (1989) by mixing 100 µl of total extract with 900 µl of acetone. The extract was then centrifuged at 15 000 g for 1 min and the supernatant was used for the subsequent assays. For Rubisco content, subsamples of the supernatant were incubated for 10 min in activation buffer [50 mM EPPS (pH 8.0), 10 mM MgCl<sub>2</sub>, 2 mM EDTA, 20 mM NaHCO<sub>3</sub>]. Rubisco content was estimated by the irreversible binding of [<sup>14</sup>C]CABP (2-C-carboxyarabinitol 1,5-bisphosphate) to the fully carbamylated enzyme (Sharwood *et al.*, 2008). Extractable soluble proteins were measured using the Pierce Coomassie Plus (Bradford) protein assay kit (Thermo Scientific, Rockford, IL, USA).

The activities of the photosynthetic enzymes Rubisco, PEPC, and NADP-ME were measured using spectrophotometric assays as described previously (Jenkins *et al.*, 1987; Ashton *et al.*, 1990; Sharwood *et al.*, 2008, 2014, 2016b; Pengelly *et al.*, 2010). Briefly, initial Rubisco activity was measured in assay buffer containing 50 mM EPPS-NaOH (pH 8), 10 mM MgCl<sub>2</sub>, 0.5 mM EDTA, 1 mM ATP, 5 mM phosphocreatine, 20 mM NaHCO<sub>3</sub>, 0.2 mM NADH, 50 U of creatine phosphokinase, 0.2 mg of carbonic anhydrase, 50 U of 3-phosphoglycerate kinase, 40 U of glyceraldehyde-3-phosphate dehydrogenase, 113 U of triose-phosphate isomerase, and 39 U

**Table 2.** Statistical summary

Parameter	Species	Treat	Species×treatment	Species (rand)	Subtype	Treatment	Subtype×treatment
Total DM (g per plant)	***	***	***	***	*	**	**
Total leaf area (m <sup>2</sup> per plant)	***	***	***	***	ns	*	*
Root/shoot DM	***	***	***	***	ns	**	ns
LMA (g m <sup>-2</sup> )	***	***	***	***	ns	*	ns
Leaf N <sub>mass</sub> (mg g <sup>-1</sup> )	***	*	***	***	ns	ns	ns
Leaf N <sub>area</sub> (gm <sup>-2</sup> )	***	***	***	**	ns	***	ns
Leaf NUE	***	***	**	***	0.10	**	*
Δ <sub>DM</sub> (%)	***	***	***	***	*	*	*
PNUE (μmol CO <sub>2</sub> s <sup>-1</sup> g <sup>-1</sup> N)	***	***	***	NA	0.10	0.07	0.06
PWUE (μmol CO <sub>2</sub> mol <sup>-1</sup> H <sub>2</sub> O)	***	*	*	***	ns	ns	ns
A <sub>h</sub> at HL (μmol m <sup>-2</sup> s <sup>-1</sup> )	***	***	***	***	0.09	**	*
A <sub>t</sub> at LL (μmol m <sup>-2</sup> s <sup>-1</sup> )	***	**	***	**	ns	*	*
g <sub>sh</sub> at HL (μmol m <sup>-2</sup> s <sup>-1</sup> )	***	***	**	***	ns	**	0.07
g <sub>sl</sub> at LL (μmol m <sup>-2</sup> s <sup>-1</sup> )	*	ns	ns	*	ns	ns	ns
Δ <sub>Ph</sub> at HL (%)	***	***	*	***	ns	0.10	ns
Δ <sub>Pl</sub> at LL (%)	***	ns	ns	***	ns	ns	ns
C/C <sub>ah</sub> at HL	***	***	0.06	***	ns	ns	ns
C/C <sub>al</sub> at LL	***	ns	*	0.07	ns	ns	ns
Leakiness ( $\Phi_h$ ) at HL	***	**	*	***	ns	**	ns
Leakiness ( $\Phi$ ) at LL	***	ns	ns	***	ns	ns	ns
R <sub>d</sub> (μmol m <sup>-2</sup> s <sup>-1</sup> )	***	***	*	**	ns	0.06	ns
IS at HL (μmol m <sup>-2</sup> s <sup>-1</sup> bar <sup>-1</sup> )	***	***	***	***	ns	*	0.10
CSR at HL (μmol m <sup>-2</sup> s <sup>-1</sup> )	***	***	***	***	0.07	**	*
IS/CSR at HL	***	ns	*	*	ns	ns	ns
A <sub>max</sub> (μmol m <sup>-2</sup> s <sup>-1</sup> )	***	***	***	NA	0.10	**	*
Φ <sub>max</sub> (mol CO <sub>2</sub> mol <sup>-1</sup> quanta)	***	***	***	***	0.08	*	*
Curvature factor ( $\theta$ )	***	0.08	***	*	0.10	0.08	*
Initial Rubisco activity	*	***	*	*	ns	*	*
Rubisco activity (μmol m <sup>-2</sup> s <sup>-1</sup> )	ns	***	ns	*	ns	*	ns
Rubisco sites (μmol m <sup>-2</sup> )	***	***	***	***	ns	*	ns
Rubisco activation (%)	***	***	***	*	ns	0.10	0.07
PEPC activity (μmol m <sup>-2</sup> s <sup>-1</sup> )	***	***	***	***	0.10	**	*
PEPC/Rubisco activity	***	***	***	***	0.08	*	*
NADP-ME activity (μmol m <sup>-2</sup> s <sup>-1</sup> )	***	***	***	NA	*	*	*
NAD-ME activity (μmol m <sup>-2</sup> s <sup>-1</sup> )	***	***	***	***	0.10	*	ns
PEP-CK activity (μmol m <sup>-2</sup> s <sup>-1</sup> )	***	***	***	***	ns	*	ns
DCs (μmol m <sup>-2</sup> s <sup>-1</sup> )	***	***	***	***	ns	*	0.10
Protein (g m <sup>-2</sup> )	*	***	***	NA	ns	*	ns

Summary of statistical analysis using two-way ANOVA to test for the effects of species and light treatment, and a linear-mixed effect model to test subtype and light treatment effects where species were considered as a random variable.

ns, not significant ( $P>0.05$ ); \* $P<0.05$ ; \*\* $P<0.01$ ; \*\*\* $P<0.001$

of glycerol-3-phosphate dehydrogenase, and the reaction initiated by the addition of 0.22 mM ribulose-1,5-bisphosphate (RuBP). For maximal Rubisco activity, the supernatant was activated in assay buffer for 10 min at 25 °C before initiation of the reaction. Rubisco activation was calculated as the initial/maximal Rubisco activity ratio. Our Rubisco activity from *in vitro* assays was slightly lower than CO<sub>2</sub> assimilation rates. Hence, in the current study, we presented Rubisco activity estimated from Rubisco sites measured with CABP assay and published Rubisco  $K_{cat}$  for individual species (Sharwood *et al.*, 2016a), and Rubisco activation values are from *in vitro* initial and activated Rubisco assays.

PEPC activity was measured in assay buffer [50 mM EPPS-NaOH (pH 8.0), 0.5 mM EDTA, 10 mM MgCl<sub>2</sub>, 0.2 mM NADH, 5 mM glucose-6-phosphate, 0.2 mM NADH, 1 mM NaHCO<sub>3</sub>, 1 U of malate dehydrogenase (MDH)] after the addition of 4 mM PEP. NADP-ME activity was measured in assay buffer [50 mM NADP-ME buffer (pH 8.3), 4 mM MgCl<sub>2</sub>, 0.5 mM NADP, 0.1 mM EDTA] after the addition of 5 mM malic acid.

The activity of PEP-CK was measured in the carboxylation direction using the method outlined previously (Kotevaya *et al.*, 2015; Sharwood *et al.*, 2016b). For PEP-CK and NAD-ME activity, a separate leaf disc was homogenized in extraction buffer containing 50 mM HEPES (pH 7.5), 2 mM EDTA, 0.05% Triton, 5 mM DTT, 1% PVPP, and 2 mM MnCl<sub>2</sub> using a 2 ml Tenbroeck glass homogenizer kept on ice. The extract was centrifuged at 21 130 g for 1 min and the supernatant used for PEP-CK and NAD-ME activity assays. PEP-CK activity was measured in assay buffer containing 50 mM HEPS (pH 6.3), 4% β-mercaptoethanol, 100 mM KCl, 90 mM KHCO<sub>3</sub>, 0.5 mM ADP, 2 mM MnCl<sub>2</sub>, 0.2 mM NADH, 6 U of MDH, and 5 mM aspartic acid after the addition of 10 mM PEP. NAD-ME activity was measured in 25 mM Tricine (pH 8.3), 5 mM DTT, 2 mM NAD, 0.1 mM acetyl-CoA, 4 mM MnCl<sub>2</sub>, and 2 mM EDTA after the addition of 5 mM malic acid. Enzyme activity was calculated by monitoring the decrease/increase of NADH<sup>+</sup> absorbance at 340 nm with a UV-VIS spectrophotometer (model 8453, Agilent Technologies Australia, Mulgrave, Victoria).

### SDS-PAGE and immunoblot analysis of photosynthetic proteins

SDS-PAGE and immunoblot analysis of photosynthetic proteins were performed as described in Sharwood *et al.* (2014). The procedures are described below.

Subsamples of total leaf extracts used for enzyme assays were mixed with 0.25 vols of 4× LDS buffer (Invitrogen) containing 100 mM DTT and placed in liquid nitrogen, then stored at -20 °C until they were analysed. For confirmatory visualization, protein samples were separated by SDS-PAGE in TGX Any kD (BioRad) pre-cast polyacrylamide gels buffered with 1× Tris-glycine SDS buffer (BioRad) at 200 V using the Mini-Protean apparatus at 4 °C. Proteins were visualized by staining with Bio-Safe Coomassie G-250 (BioRad) and imaged using the VersaDoc imaging system (BioRad).

For immunoblot analyses, samples of total leaf proteins were separated by SDS-PAGE as outlined above, then transferred at 4 °C to nitrocellulose membranes (0.45 µm; BioRad) using the Xcell Surelock western transfer module (Invitrogen) buffered with 1× Transfer buffer [20 × 25 mM Bicine, 25 mM Bis-Tris, 1 mM EDTA, 20% (v/v) methanol]. After 1 h transfer at 30 V, the membrane was placed in blocking solution [3% (w/v) skim milk powder in Tris-buffered saline (TBS); 50 mM Tris-HCl pH 8, 150 mM NaCl] for 1 h at room temperature with gentle agitation.

Primary antisera raised in rabbit against tobacco Rubisco (prepared by S.M. Whitney) was diluted 1:4000 in TBS before incubation for 1 h with membranes at room temperature with gentle agitation. Antiserum raised against PEPC (Cat. AS09 458) was obtained from AgriSera and diluted 1:2000 with TBS. For NADP-ME and PEP-CK, synthetic peptides based on monocot amino acid sequences for each protein were synthesized by GL Biochem and antisera were raised against each peptide in rabbits. The reactive antiserum was the antigen purified for use in immunoblot analysis (GL Biochem). The NADP-ME and PEP-CK antisera were diluted in TBS 1:1000 and 1:500, respectively. All primary antisera were incubated with membranes at room temperature for 1 h with gentle agitation before washing three times with TBS. Secondary goat anti-rabbit antiserum conjugated to horseradish peroxidase (HRP; Cat. NEF 812001EA, Perkin Elmer) was diluted 1:3000 in TBS and incubated with the membranes for 1 h at room temperature followed by three washes with TBS. Immunoreactive peptides were detected using the Immun-Star Western C kit (Cat. 170-5070, BioRad) and imaged using the VersaDoc.

### Leaf nitrogen and carbon isotope analyses

Following gas exchange and leaf disc sampling, the remainder of the LFEL was cut and its area was measured using a leaf area meter (LI-3100A, LI-COR). The LFEL was oven-dried, weighed, then milled to a fine powder. Leaf N content was determined on the ground leaf tissue samples using a CHN analyser (LECO TruSpec, LECO Corp., MI, USA). Leaf mass per area (LMA, g m<sup>-2</sup>) was calculated as total leaf dry mass/total leaf area. Leaf N per unit area (N<sub>area</sub>) was calculated as (mmol N g<sup>-1</sup>) × LMA (g m<sup>-2</sup>). For leaf δ<sup>13</sup>C, ground leaf samples were combusted in a Carlo Erba Elemental Analyser (Model 1108) and the released CO<sub>2</sub> was analysed by MS. The δ<sup>13</sup>C = [(R<sub>sample</sub> - R<sub>standard</sub>) / R<sub>standard</sub>] × 1000, where R<sub>sample</sub> and R<sub>standard</sub> are the <sup>13</sup>C/<sup>12</sup>C ratio of the sample and standard (Pee Dee Belemnite), respectively. Photosynthetic carbon isotope discrimination based on leaf dry matter δ<sup>13</sup>C (Δ<sub>DM</sub>) was calculated as described by Farquhar and Richards (1984):

$$\Delta_{DM} = \frac{\delta_a - \delta_p}{1 + \delta_p} \quad (11)$$

where δ<sub>a</sub> and δ<sub>p</sub> are the δ<sup>13</sup>C values in the glasshouse air (assumed to be -8‰) and in the leaf bulk material, respectively.

### PWUE and PNUE calculations

Photosynthetic water use efficiency (PWUE) was calculated as A (µmol m<sup>-2</sup> s<sup>-1</sup>) / g<sub>s</sub> (mol m<sup>-2</sup> s<sup>-1</sup>). Photosynthetic nitrogen use efficiency (PNUE) was calculated as A (µmol m<sup>-2</sup> s<sup>-1</sup>) / leaf N<sub>area</sub> (mmol m<sup>-2</sup>).

### Plant harvest

Plants were harvested 10–11 weeks after transplanting. At harvest, leaves were separated from stems. Total leaf area was determined using a Licor LI-3100A leaf area meter. Roots were washed free of soil. Plant materials were oven-dried at 80 °C for 48 h before dry mass (DM) was measured. Total plant DM included leaf, stem, and root DM. Leaf nitrogen use efficiency (NUE) was calculated as the ratio of total plant DM (g per plant)/total leaf N content (mg).

### Statistical analysis

Growth, gas exchange, enzyme assay, and leaf nitrogen analyses were performed on 3–4 replicates per treatment combination (species × light). For species as a main effect, the relationship between various response variables and the main effect (species and light treatment) and their interactions were fitted using the linear model in R (R Foundation for Statistical Computing, Vienna, Austria) (R Core Team, 2015). Since the numbers of species within each subtype were unequal and measurements were taken on multiple individuals within a species, each unit cannot be considered as a true independent replicate. Therefore, a linear mixed effect model (lmer) was used to estimate the fixed effect associated with light treatment and subtype, where species were treated as a random variable. For each response variable, the models containing all possible fixed effects were fitted using the lme4 package (Bates *et al.*, 2013) in R. The model residues were tested for normality, and data transformation was carried out to achieve a normal distribution, if required. Significance tests were performed with a parametric bootstrap by using the 'pbkrtest' package in R (Halekoh and Højsgaard, 2014). Briefly, a linear mixed effect model (fitted with maximum likelihood), full and restricted models, was used as a sample to generate the likelihood ratio statistic (LRT) after 1000 bootstraps. To estimate the P-value, LRT divided by the number of degrees of freedom was assumed to be F-distributed where denominator degrees of freedom are determined by matching the first moment of reference distribution.

## Results

Throughout this study, the species effect was highly significant for all parameters and generally is not described below (Table 2).

### Plant growth and leaf chemistry

Across treatments, PEP-CK species had a higher average plant DM and total leaf area relative to NADP-ME and NAD-ME species (P < 0.05; Table 2; Fig. 1A; Supplementary Table S1). Shade reduced plant DM to a greater extent in NAD-ME (~95%) and PEP-CK (~92%) relative to NADP-ME (~81%) species (Table 2; Fig. 1A; Supplementary Table S1). Total plant DM and total leaf area were linearly correlated across the species and light treatments ( $R^2=0.9$  for the log relationship) (Fig. 1C). The effect of shading on plant DM and leaf area increased linearly with shaded plant DM ( $R^2=0.97$  and 0.89, respectively). The root to shoot ratio did not vary according to subtype but was substantially reduced by shade

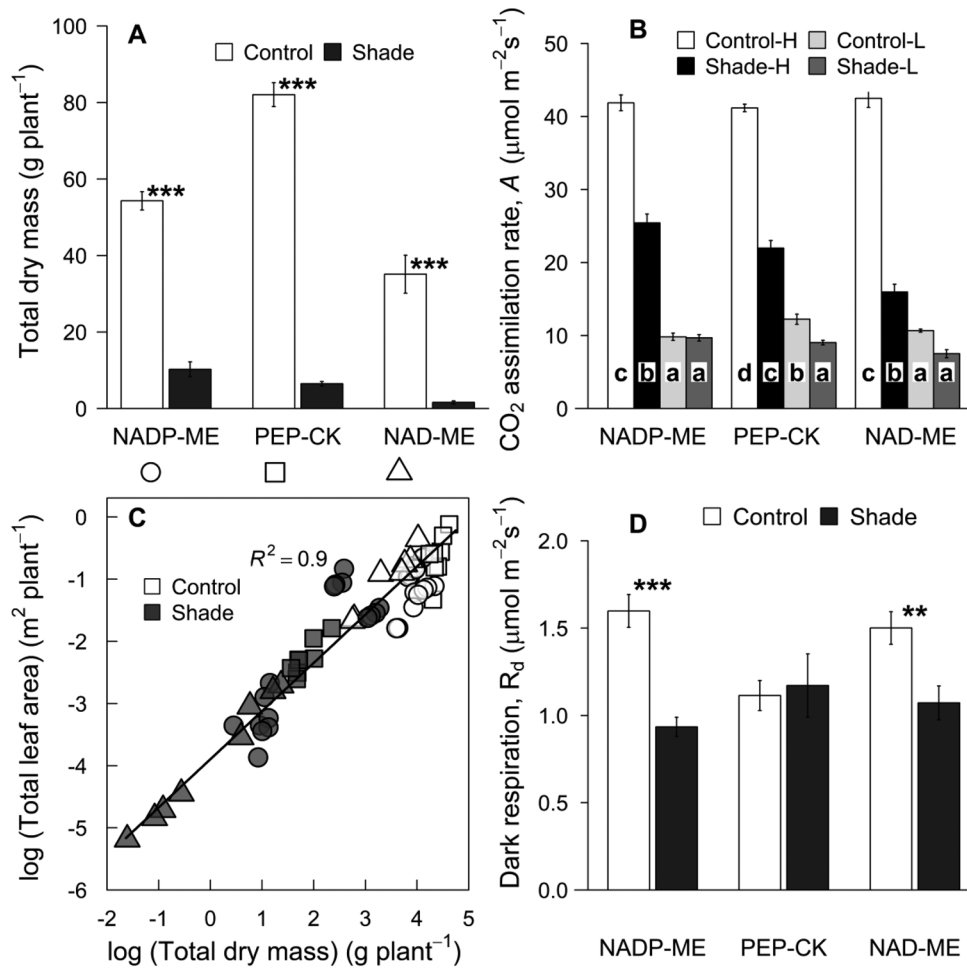


**Fig. 1.** Total plant dry mass and leaf area. (A) Total plant dry mass (DM), (B) CO<sub>2</sub> assimilation rate measured at ambient [CO<sub>2</sub>], (C) relationship between the log of total leaf area and the log of total DM, and (D) dark respiration ( $R_d$ ) for eight C<sub>4</sub> grasses belonging to three biochemical subtypes and grown in control (full sunlight; white) or shade (16% of natural sunlight; black) environments. Each column represents the mean  $\pm$ SE of subtype. For (A) and (D), statistical significance levels (*t*-test) for the growth condition within each subtype are shown: \**P*<0.05; \*\**P*<0.01; \*\*\**P*<0.001. In (B), measurements were made at 2000 (HL) and 250 (LL) μmol quanta m<sup>-2</sup> s<sup>-1</sup> for both control and shade treatments. Letters indicate the ranking (from lowest=a) within each subtype using multiple-comparison Tukey's post-hoc test.

in all species (Table 2; Supplementary Table S1). There was no significant subtype effect on LMA, leaf N<sub>mass</sub>, or leaf N<sub>area</sub>, while shade reduced LMA and leaf N<sub>area</sub> (but not leaf N<sub>mass</sub>) in most species (Table 2; Supplementary Table S1).

#### Leaf gas exchange at low and high light

Overall, there was no significant subtype effect on CO<sub>2</sub> assimilation rates and stomatal conductance measured at HL ( $A_h$  and  $g_{sh}$ , respectively) and LL ( $A_l$  and  $g_{sl}$ , respectively) (*P*>0.05, Table 2). However, there was a significant treatment and subtype×treatment effect on both  $A_h$  and  $A_l$  (*P*<0.05; Table 2). In particular, shade reduced  $A_h$  and  $A_l$  to a greater extent in NAD-ME (−62% and −27%, respectively) relative to PEP-CK (−46% and −15%, respectively) and NADP-ME (−40% and 0%, respectively) species (Fig. 1B; Supplementary Table S2). Furthermore, under shade, NADP-ME species had the highest and NAD-ME species had the lowest  $A_h$  and  $g_{sh}$ , indicating that photosynthesis and stomatal conductance acclimated to shade more strongly in the latter species (Fig. 1B; Supplementary Table S2). The CO<sub>2</sub> assimilation rate

was strongly correlated with stomatal conductance across all species and treatments ( $R^2=0.86$ ) (Fig. 2A). Consequently,  $C_i/C_a$  was constant and, together with PWUE, did not vary according to the subtype or light treatment (Table 2; Supplementary Table S2).

$R_d$  did not differ between the subtypes but it was reduced by shade in NADP-ME and NAD-ME species (Fig. 1D; Table 2; Supplementary Table S2). For control plants, the  $R_d/A$  ratio (measured at growth light) was lowest in PEP-CK species; shade increased  $R_d/A$  less in NADP-ME (+158%) relative to PEP-CK (+374%) and NAD-ME (+341%) species (Table 2; Supplementary Table S2). CO<sub>2</sub> assimilation rate measured at HL,  $A_h$ , and  $R_d$  showed good linear relationships to leaf N<sub>area</sub> across species ( $R^2=0.59$  and  $R^2=0.54$ , respectively). PNUE was marginally lower (*P*=0.1) in NAD-ME relative to NADP-ME and PEP-CK species, and was reduced by shade mostly in NAD-ME (−28%) and PEP-CK (−19%) (Table 2; Supplementary Table S2). Leaf NUE was reduced to a greater extent in NADP-ME and NAD-ME species (−41% and −39%, respectively) relative to PEP-CK species (Table 2; Supplementary Table S1).

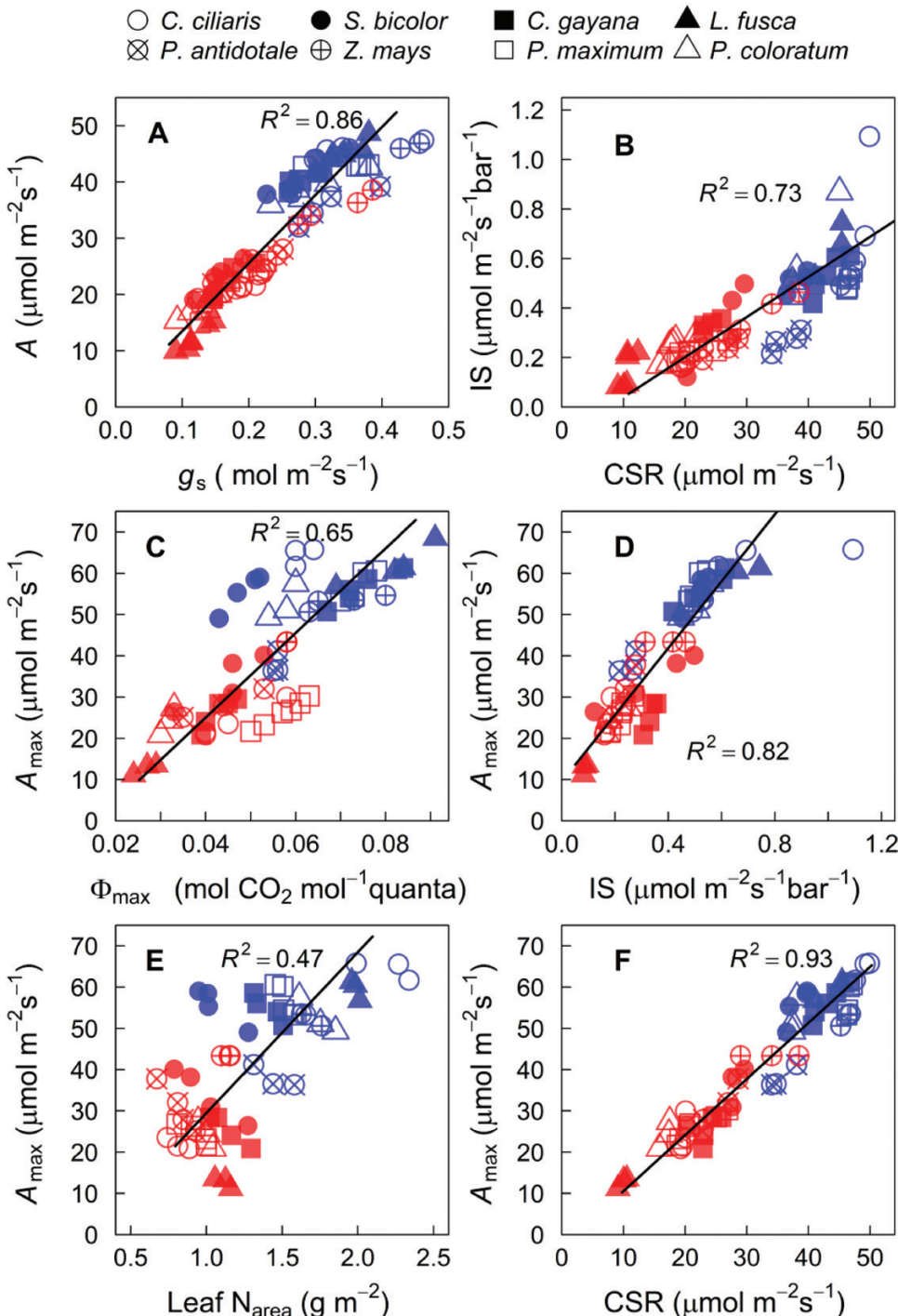


**Fig. 2.** Relationships among physiological and *in vivo* derived parameters. CO<sub>2</sub> assimilation ( $A_h$ ), stomatal conductance ( $g_s$ ), IS, and CSR derived from  $A-C_i$  curves measured at high light,  $A_{\max}$  and  $\Phi_{\max}$  derived from light response curves measured at saturating [CO<sub>2</sub>], and leaf N<sub>area</sub> for eight C<sub>4</sub> grasses belonging to three biochemical subtypes grown in control (full sunlight; blue) or shade (16% of natural sunlight) (red) environments. Straight lines are linear regressions for all data points.

#### Photosynthetic CO<sub>2</sub> response curves

The initial slopes (ISs) of the  $A-C_i$  curves and CO<sub>2</sub>-saturated rates (CSRs) were estimated from measurements at HL (Supplementary Fig. S2). In control plants, the IS and CSR did not vary with subtypes, but were reduced by shade to a greater extent in NAD-ME (~77% for IS and ~64% for CSR) than PEP-CK (~49% for IS and CSR) and NADP-ME species (~46% for IS and ~39% for CSR) (Tables 2, 3). Consequently,

CSR of shaded plants was lowest in NAD-ME, intermediate in PEP-CK, and highest in NADP-ME species (Tables 2, 3). There was a strong linear relationship between IS and CSR irrespective of treatment and subtype ( $R^2=0.73$ ) (Fig. 2B).

#### Photosynthetic light response curves

The light-saturated photosynthesis rate,  $A_{\max}$ , and photosynthetic quantum yield,  $\Phi_{\max}$ , were estimated from the light

response curves of photosynthesis measured at saturating CO<sub>2</sub> (Supplementary Fig. S3). In control plants,  $A_{\max}$  and  $\Phi_{\max}$  did not vary with subtypes (Tables 2, 3; Fig. 3G). Shade reduced  $A_{\max}$  and  $\Phi_{\max}$  to a greater extent in NADP-ME species ( $-68\%$  and  $-55\%$ , respectively) than PEP-CK ( $-54\%$  and  $-32\%$ , respectively) and NADP-ME ( $-39\%$  and  $-19\%$ ,

respectively) species (Tables 2, 3). Consequently,  $\Phi_{\max}$  was lower in shaded NADP-ME species relative to their NADP-ME and PEP-CK counterparts ( $P < 0.05$ ), which indicates differential shade acclimation of photosynthetic capacity and quantum efficiency among the C<sub>4</sub> subtypes. In control plants, the curvature ( $\theta$ ) was highest in NADP-ME (0.81) and lowest

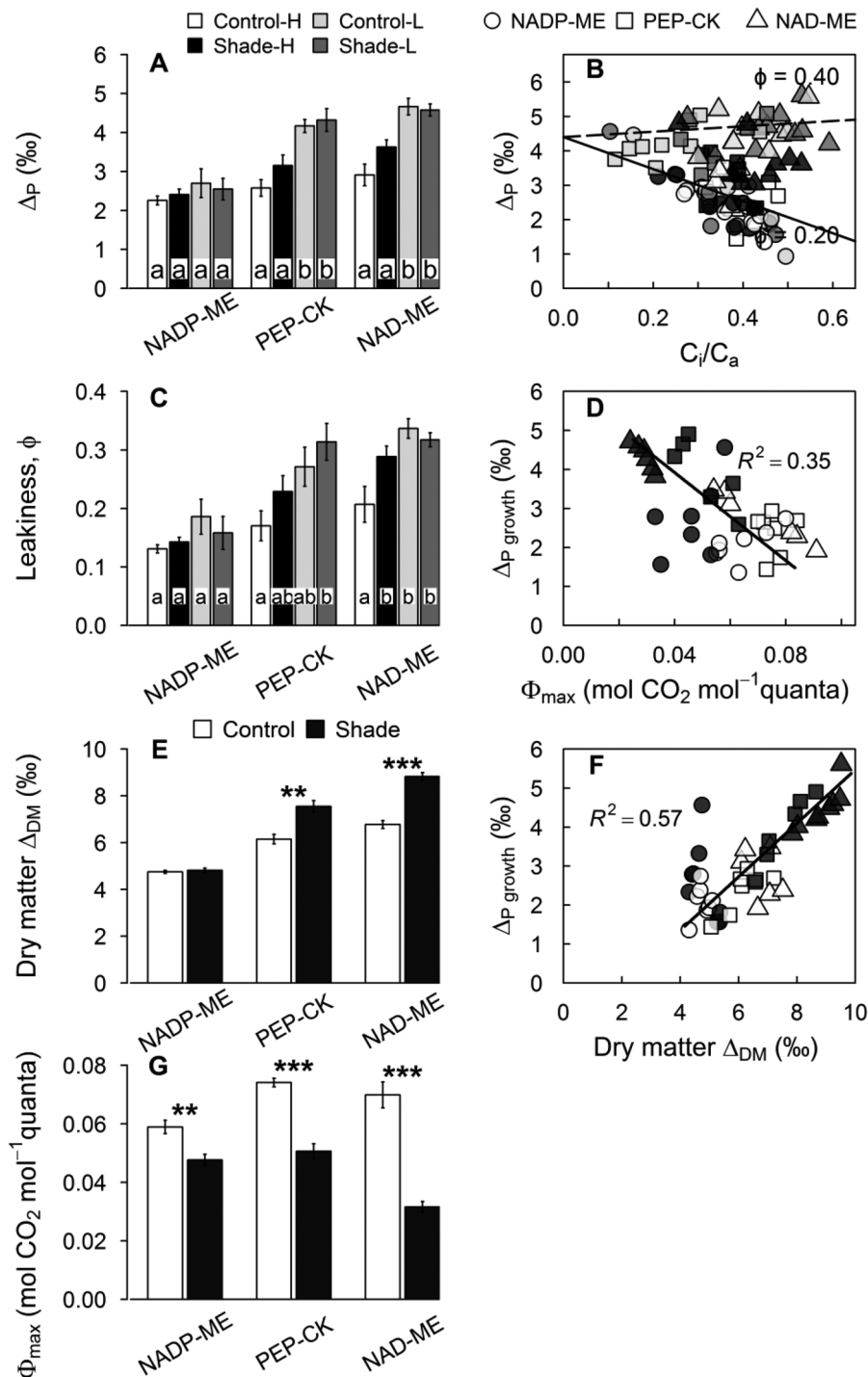


**Fig. 3.** The CCM efficiency parameters. (A) Photosynthetic carbon isotope discrimination ( $\Delta_P$ ) measured concurrently with leaf gas exchange, (B) carbon isotope discrimination against the ratio of intercellular [CO<sub>2</sub>] to ambient [CO<sub>2</sub>] ( $C_i/C_a$ ), (C) leakiness ( $\phi$ ) at measured light (h or l), (D)  $\Delta_P$  measured at growth light ( $\Delta_{\text{growth}}$ ) against  $\Phi_{\max}$ , (E)  $\Delta_{\text{DM}}$  calculated from leaf dry matter  $\delta^{13}\text{C}$ , (F)  $\Delta_P$  measured at growth light ( $\Delta_{\text{growth}}$ ) against  $\Delta_{\text{DM}}$ , and (G) and maximum quantum yield of PSII,  $\Phi_{\max}$ , for C<sub>4</sub> grasses belonging to three biochemical subtypes grown in control (full sunlight; white) or shade (16% of natural sunlight; black) environments. Each column represents the mean  $\pm$ SE of subtype. Statistical significance levels (t-test) for the growth condition within each subtype are shown: \* $P < 0.05$ ; \*\* $P < 0.01$ ; \*\*\* $P < 0.001$ .

in NAD-ME species (0.53) ( $P<0.05$ ) (Tables 2, 3). When all data were considered,  $A_{\max}$  was well correlated with  $\Phi_{\max}$ , IS, CSR, and leaf N<sub>area</sub> (Fig. 2C–F).

#### Carbon isotope discrimination

Concurrent measurements of  $^{13}\text{CO}_2/^{12}\text{CO}_2$  discrimination and leaf gas exchange showed that photosynthetic carbon isotope discrimination,  $\Delta_p$ , was independent of the C<sub>4</sub> subtype at HL (Table 2).  $\Delta_p$  tended to be lower in NADP-ME species relative to the other two subtypes, but differences were not significant, except when compared with the control plants measured at HL (Table 2; Supplementary Table S3). For NADP-ME species,  $\Delta_p$  was unchanged by either LL or shade, while  $\Delta_p$  increased in PEP-CK and NAD-ME species in response to both LL and shade (22–37%) (Fig. 3A; Supplementary Table S3).

Leakiness ( $\phi$ ) ranged between 0.15 and 0.35 across the C<sub>4</sub> grasses and light treatments (Fig. 3B, C). For shaded plants measured at HL, NAD-ME species had higher leakiness (0.29) than NADP-ME species (0.14) (Supplementary Table S3). Overall, NAD-ME species exhibited increased  $\phi$  at LL and in the shade environment (Fig. 3C; Supplementary Table S3).

Photosynthetic carbon isotope discrimination derived from bulk leaf  $\delta^{13}\text{C}$  values,  $\Delta_{\text{DM}}$ , was significantly lower in NADP-ME species relative to the other two subtypes ( $P<0.05$ ) (Table 2; Supplementary Table S3). Shade increased  $\Delta_{\text{DM}}$  in NAD-ME and PEP-CK species only (+30% and +22%, respectively) (Fig. 3E; Table 2; Supplementary Table S3).

There was a strong linear relationship between photosynthetic discrimination measured at growth light,  $\Delta_{\text{growth}}$ , and  $\Delta_{\text{DM}}$  ( $R^2=0.56$ ) (Fig. 3F). This relationship had an x-intercept of 0.9‰, which reflects the difference between  $\Delta_{\text{growth}}$  and  $\Delta_{\text{DM}}$  due to time-integrated changes in ambient  $^{13}\text{CO}_2/^{12}\text{CO}_2$  and post-photosynthetic fractionation. The good fit between  $\Delta_{\text{growth}}$  and  $\Delta_{\text{DM}}$  suggests that leaf  $\delta^{13}\text{C}$  is a good predictor of  $\Delta_{\text{growth}}$ , and perhaps  $C_i/C_a$  (PWUE) for C<sub>4</sub> grasses when changes are caused by a difference in light intensity. In addition, there was a significant, negative linear relationships between  $\Phi_{\max}$  and  $\Delta_{\text{growth}}$  ( $R^2=0.35$ ) (Fig. 3D).

#### Activity of photosynthetic enzymes

Control NAD-ME plants had the highest leaf content of Rubisco sites ( $P<0.05$ ) (Fig. 4A; Table 2; Supplementary Table S4). Rubisco activation decreased significantly in NAD-ME (~40%) and PEP-CK (~22%) species, while it increased by ~15% in NADP-ME species (subtype  $\times$  light  $P=0.07$ ) (Fig. 4A, B; Table 2; Supplementary Table S4). Consequently, initial Rubisco activity did not differ according to the C<sub>4</sub> subtype ( $P>0.05$ ), and was reduced to a greater extent in NAD-ME relative to the PEP-CK and NADP-ME species under shade in all C<sub>4</sub> grasses (subtype  $\times$  treatment  $P<0.08$ ) (Fig. 4C; Table 2; Supplementary Table S4). Soluble protein content decreased under shade by 12–67% depending on the species but not the subtype (Table 2; Supplementary Table S4).

In general, shade reduced PEPC activity by 49–84% in the C<sub>4</sub> grasses. PEPC activity was higher in control NADP-ME

plants and decreased to a lesser extent in NAD-ME (66%) than in NADP-ME (69%) and PEP-CK (65%) species (Fig. 4D; Table 2; Supplementary Table S4). Consequently, shade reduced the ratio of PEPC to initial Rubisco activity in NADP-ME (~44%) but not in PEP-CK (~3%) species, while this ratio tended to increase in NAD-ME species (+30%) (Fig. 4E; Supplementary Table S4).

There was a significant relationship between the PEPC/initial Rubisco activity ratio and  $\Delta_{\text{DM}}$  ( $P<0.05$ ), and this relationship was stronger in shade ( $R^2=0.49$ ) than in control ( $R^2=0.40$ ) plants. In contrast, PEPC/initial Rubisco activity showed a weaker relationship to  $\Delta_{\text{growth}}$  ( $R^2=0.23$ ) irrespective of treatment and subtype.

Activities of NADP-ME, PEP-CK, and NAD-ME enzymes were dominant in their respective subtype; however, substantial PEP-CK activity (6–25  $\mu\text{mol m}^{-2} \text{s}^{-1}$ ) was measured in NADP-ME and NAD-ME species (Supplementary Table S4). Shade reduced the activity of NADP-ME, PEP-CK, and NAD-ME by 35–60, 52–64, and 49–57%, respectively ( $P<0.05$ ). Shade also reduced the activity of total decarboxylases by 25–64% ( $P<0.05$ ); the reduction was lower in NADP-ME (42%) relative to PEP-CK (60%) and NAD-ME (65%) species (Fig. 4F; Table 2; Supplementary Table S4).

The detectability of enzyme activity was corroborated by immunodetection of the corresponding protein for all the photosynthetic enzymes assayed, except for NAD-ME where a suitable antibody was not available during this study (Fig. 5). Rubisco and PEPC proteins were detected in all species and treatments. Surprisingly, NADP-ME protein was detected in all C<sub>4</sub> species, including NAD-ME and PEP-CK. This may be attributed to cross-reaction with a non-photosynthetic isomer of NADP-ME or NAD-ME proteins (Fig. 5). PEP-CK protein was strongly detectable in *Panicum maximum* and to a lesser extent in *Chloris gayana*, although *C. gayana* had the highest PEP-CK activity (Fig. 5; Supplementary Table S4). In addition, PEP-CK protein was detected in three NADP-ME species, but not in *Sorghum bicolor*, reflecting well the trends in PEP-CK activity (Fig. 5; Supplementary Table S4).

## Discussion

C<sub>4</sub> photosynthesis is thought to be less plastic in response to shade than C<sub>3</sub> photosynthesis due to its complex anatomy and biochemistry (Sage and McKown, 2006). Yet, some studies found similar photosynthetic responses to LL in C<sub>3</sub> and C<sub>4</sub> plants (Tazoe et al., 2006, 2008; Pengelly et al., 2010). These studies have focused on the response of selected C<sub>4</sub> species to short-term changes in irradiance (Tazoe et al., 2008; Pengelly et al., 2010; Ubierna et al., 2013; Bellasio and Griffiths, 2014a, b) or long-term adaptation to growth under LL (Kromdijk et al., 2008, 2010; Tazoe et al., 2008; Bellasio and Griffiths, 2014b). However, there is limited information about how LL responses differ across the C<sub>4</sub> subtypes. Here, we present the first study comparing the short- and long-term responses to LL of C<sub>4</sub> grasses with different biochemical subtypes. We hypothesized that (i) LL (short and long term) will compromise the CCM efficiency to a greater extent in NAD-ME than

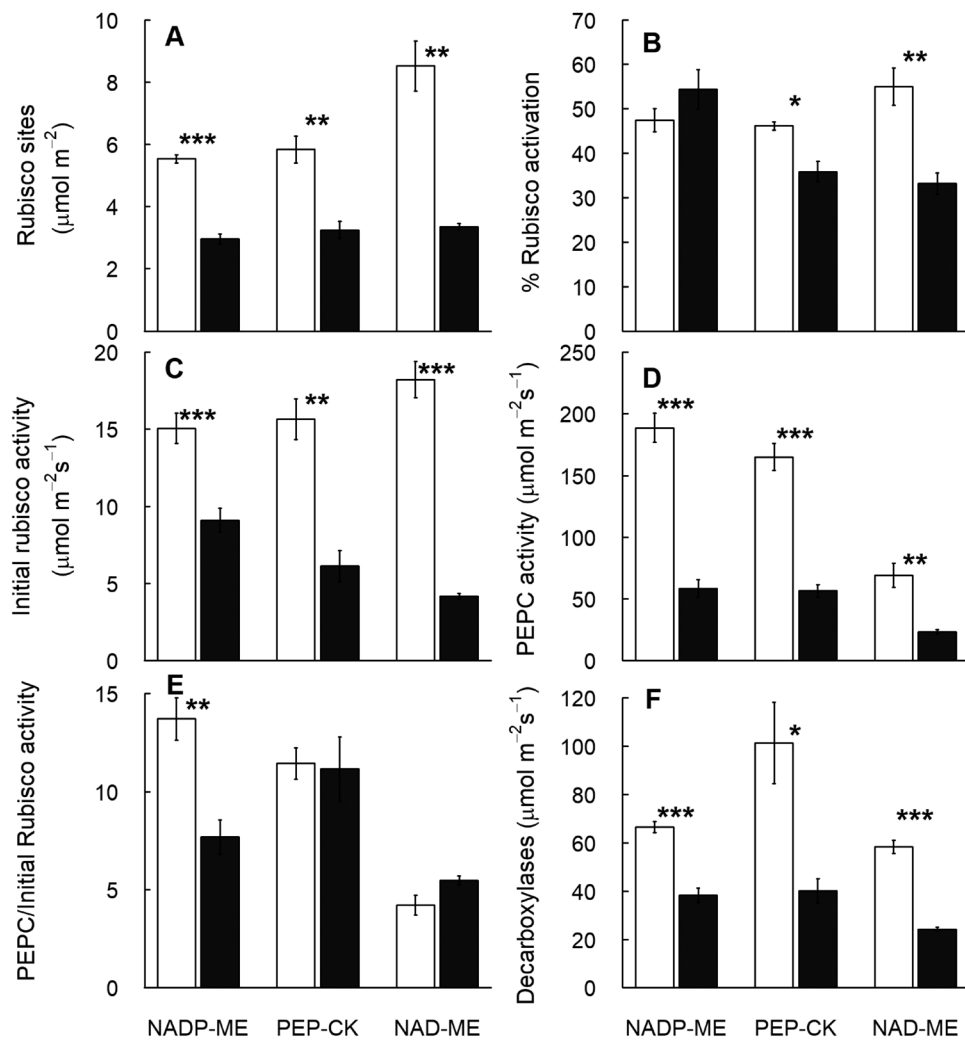


**Fig. 4.** Shade acclimation of photosynthetic enzymes in C<sub>4</sub> subtypes. (A) Rubisco sites, (B) % Rubisco activation, (C) Initial Rubisco activity, (D) PEPC activity, (E) PEPC to initial Rubisco activity ratio, and (F) decarboxylases activity for eight C<sub>4</sub> grasses belonging to three biochemical subtypes and grown in control (full sunlight; white) or shade (16% of natural sunlight; black) environments. Each column represents the mean  $\pm$  SE of subtype. Statistical significance levels (*t*-test) for the growth condition within each subtype are shown: \**P*<0.05; \*\**P*<0.01; \*\*\**P*<0.001.

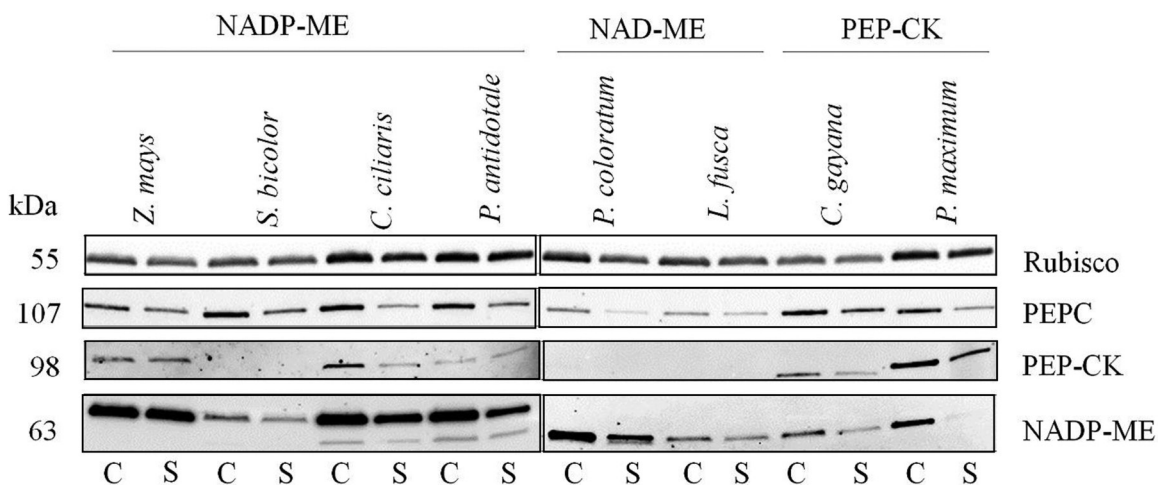


**Fig. 5.** Immunoblot analysis of photosynthetic enzymes. Immunoblot analysis for the photosynthetic proteins Rubisco, PEPC, PEP-CK, and NADP-ME extracted from leaves of eight C<sub>4</sub> grasses belonging to three biochemical subtypes in control (C) or shade (S) environments. Loaded volumes varied between 4  $\mu\text{l}$  and 15  $\mu\text{l}$  in order to normalize the protein content to a common leaf area. Because of the small gel size, a limited number of samples (8–9) was loaded on an individual gel. Finally, all immunoblots of the studied protein and species were arranged in a composite figure. For uniform visualization, gamma settings of individual images were adjusted. A protein ladder was used for individual immunoblots; for simplicity, band size is referred to numerically.

in PEP-CK or NADP-ME grasses due to a greater increase in leakiness ( $\phi$ ) in the former subtype; and (ii) shade will cause a greater photosynthetic acclimation in NADP-ME grasses than in NADP-ME and PEP-CK counterparts by virtue of their higher leaf N and Rubisco content. To evaluate these hypotheses, we grew eight C<sub>4</sub> grasses belonging to three biochemical subtypes (NADP-ME, NAD-ME, and PEP-CK) under shade (16% sunlight) or control (full sunlight) conditions, and subsequently measured their photosynthetic characteristics under both LL and HL. Our results supported both hypotheses and demonstrated that LL compromised the CCM efficiency and photosynthetic quantum yield to a greater extent in NAD-ME relative to PEP-CK and NADP-ME species.

#### *Low light compromised the CCM efficiency most in NAD-ME followed by PEP-CK, but not in NADP-ME grasses*

For the operational CCM, the C<sub>4</sub> cycle must be faster than the C<sub>3</sub> cycle (i.e. PEPC/initial Rubisco activity ratio >1) to concentrate CO<sub>2</sub> inside the BSCs, some of which will inevitably leak back out to the MCs. In the short term, LL may compromise CCM efficiency by affecting the activity of the C<sub>3</sub> cycle (e.g. Rubisco) more significantly than that of the C<sub>4</sub> cycle (e.g. PEPC) and, hence, increasing  $\Delta_P$ ,  $\phi$ , and  $\Phi_{\max}$ . Under LL,  $A$  is low and CO<sub>2</sub> evolved during respiration can make an important contribution to the total CO<sub>2</sub> concentration inside the BSCs. Larger  $R_d/A$  ratios under LL can potentially lead to higher  $\Delta_P$ . Increased  $\Delta_P$  due to respiratory CO<sub>2</sub> does not involve an energy cost for the CCM but may lead to an overestimation of  $\phi$  independently of  $\Phi_{\max}$ . Long-term acclimation to LL may act to optimize CCM efficiency by reversing the negative short-term effects of LL (Bellasio and Griffiths, 2014a). Hence, we used the metrics PEPC/initial Rubisco activity,  $R_d/A$ ,  $\phi$ , and  $\Phi_{\max}$  to evaluate the effects of LL during measurements and growth on the CCM efficiency of the various C<sub>4</sub> subtypes. Consequently, increased  $\phi$ , PEPC/initial Rubisco activity, and  $R_d/A$  can be interpreted as a less efficient photosynthetic process. Assuming that bundle sheath conductance does not change with irradiance, increased  $\Delta_P$  and  $\phi$  can be interpreted as a less efficient CCM and an indication of imbalance between the C<sub>3</sub> and C<sub>4</sub> cycles (von Caemmerer, 2000).

#### *Response of NADP-ME grasses to LL*

In the NADP-ME grasses,  $\Delta_P$ ,  $\Delta_{DM}$ , and  $\phi$  were not significantly impacted by LL during either measurement or growth (Fig. 3A, C, E), suggesting that in this subtype, the co-ordination between the C<sub>3</sub> and C<sub>4</sub> cycles was largely maintained despite changes in the light environment. Our results are in agreement with previous reports that  $\Delta_P$  was insensitive to LL during the measurements for NADP-ME species (Henderson et al., 1992; Kubásek et al., 2007; Cousins et al., 2008) as well as  $\Delta_{DM}$  being insensitive to growth under shade in NADP-ME *Zea mays* (Sharwood et al., 2014). NADP-ME species grown under shade had lower PEPC/initial Rubisco activity (-44%) and higher  $R_d/A$  (+158% at growth light) than the control plants. Decreased PEPC/initial Rubisco activity is expected to reduce  $\Delta_P$ ,  $\Delta_{DM}$ , and  $\phi$ , while increased  $R_d/A$  will have the opposite

effect under shade. The combined opposing effects may explain the insensitivity of  $\Delta_P$ ,  $\Delta_{DM}$ , and  $\phi$  in response to the shade environment. In line with this conclusion, NADP-ME species showed the lowest reduction in  $\Phi_{\max}$  (-19%), and it is likely that the contribution from photorespiration was negligible in the low-O<sub>2</sub>-evolving BSC chloroplasts of NADP-ME species (Ghannoum et al., 2005). Previous work describing the shade acclimation of the NADP-ME of *Z. mays* suggested that this species reduced the ATP cost of the CCM under shade by reducing the PEPC activity more than the C<sub>3</sub> cycle activity, which resulted in low  $\phi$  values (Bellasio and Griffiths, 2014a). Our findings support this argument by providing direct measurements of *in vitro* C<sub>4</sub> and C<sub>3</sub> cycle enzymes as well as  $\Phi_{\max}$ . This argument is also supported by the modelling approach of Wang et al. (2014) who suggested that the NADP-ME biochemical pathway is favoured at LL. In contrast to our results, differential responses of C<sub>4</sub> and C<sub>3</sub> cycle enzymes were reported in earlier studies with NADP-ME species (Sugiyama et al., 1984; Ward and Woolhouse, 1986a; Sharwood et al., 2014). This discrepancy may be related to differences in the intensity of the shade treatment used. In addition, these studies considered total (rather than initial) Rubisco activity for calculating the PEPC/Rubisco activity ratio.

It is worth noting that, in addition to NADP-ME decarboxylase activity, *Z. mays* and *Cenchrus ciliaris* showed significant activity of PEP-CK decarboxylase (16–25 µmol m<sup>-2</sup> s<sup>-1</sup>), while *S. bicolor* and *Panicum antidotale* appeared as true NADP-ME types. Without considering cytosolic resistance of BSCs to CO<sub>2</sub>, Wang et al. (2014) suggested the possibility of higher leakiness in the C<sub>4</sub> photosynthesis model with mixed decarboxylase pathways. This was not validated in our study. Bellasio and Griffiths (2014c) also suggested that the engagement of the secondary PEP-CK pathway in an NADP-ME species enables the CCM to regulate an optimal BSC [CO<sub>2</sub>] under changing light conditions. These predictions were indirectly validated in our study. Under LL, *Z. mays* showed higher  $\Delta_P$  and  $\phi$  but similar  $\Phi_{\max}$  relative to the other two NADP-ME species, *P. antidotale* and *S. bicolor* (Supplementary Table S4). However, the link between  $\Delta_P$ , CCM efficiency, and PEP-CK activity as a secondary decarboxylase in NADP-ME species requires further investigation.

#### *Response of PEP-CK and NAD-ME grasses to LL*

PEP-CK and NAD-ME plants had larger  $\Delta_{DM}$  under shade relative to the control condition (Fig. 3E). Previous studies have shown similar  $\Delta_{DM}$  responses to shade across the C<sub>4</sub> subtypes (Buchmann et al., 1996; Tazoe et al., 2006). In PEP-CK and NAD-ME grasses, instantaneous measurements of  $\Delta_P$  and  $\phi$  increased at LL, and the difference between the light treatments was highly significant when the comparison was made between control and shade plants measured under their respective growth irradiance (Fig. 3A, C). These results indicate that LL resulted in a less efficient CCM in PEP-CK and NAD-ME grasses. Additionally, the relative increase in  $\phi$  from HL to LL was larger for control (+60%) than shade (+12%) plants. This is in line with Tazoe et al. (2008) and suggests that a degree of acclimation to the shade condition mitigated the negative effects of LL observed in response to

short-term light changes during measurements. Our results with PEP-CK and NAD-ME grasses are in agreement with previous reports of increased  $\Delta_P$  and  $\phi$  with short-term exposure to LL (Henderson *et al.*, 1992; Cousins *et al.*, 2008).

In NAD-ME species, shade increased the PEPC/initial Rubisco activity (+30%) and  $R_d/A$  (+341% at growth light) and decreased  $\Phi_{max}$  (−55%). Species of the NAD-ME subtype possess significant PSII activity in the BSC (Ghannoum *et al.*, 2005), and hence potentially high [O<sub>2</sub>]. PEP-CK species exhibited intermediate responses to shade relative to the other two subtypes. In PEP-CK species, the PEPC/initial Rubisco activity ratio was not affected by shade, but the  $R_d/A$  ratio was larger (+374%) in shade than in control plants (Supplementary Table S2). Further, the reduction of  $\Phi_{max}$  under shade was intermediate in PEP-CK species (−32%) relative to NADP-ME (−19%) and NAD-ME (−55%). We also have evidence that PEP-CK species possess significant PSII activity in BSCs (Pinto, 2015). Accordingly,  $\Delta_P$ ,  $\Delta_{DM}$ , and  $\phi$  increased under shade in PEP-CK species to a similar extent relative to NAD-ME counterparts (Fig. 3A, C, E). Thus, in line with the first hypothesis, our results demonstrated that LL compromised the CCM efficiency of NAD-ME species more than that of PEP-CK species, while CCM efficiency was largely maintained in NADP-ME species under LL.

#### *Shade induced larger photosynthetic down-regulation in NAD-ME relative to NADP-ME and PEP-CK species*

In the current study, shade down-regulated  $A_h$  and light-saturated photosynthesis,  $A_{max}$ , in NAD-ME (−68%) to a greater extent than in PEP-CK (−54%) and NADP-ME (−39%) species, indicating stronger photosynthetic acclimation to shade

in the former subtype (Table 3). Shade equally reduced PEPC activity in all the C<sub>4</sub> subtypes (−68%), while Rubisco sites and activation were more profoundly reduced in NAD-ME (−60% and −40%, respectively) relative to the PEP-CK (−48% and −22%, respectively) and NADP-ME (−47% and +15%, respectively) species (Supplementary Table S4). Similar large reductions in Rubisco content and activity (>55%) were reported in studies using C<sub>3</sub> species (Evans, 1988). In shade-grown C<sub>4</sub> species, inconsistent changes in Rubisco content and activity have been observed (Winter *et al.*, 1982; Ward and Woolhouse, 1986a, b; Tazoe *et al.*, 2006), with an average reduction of 29% (Sage and McKown, 2006). A relevant study by Ward and Woolhouse (1986a) subjecting C<sub>4</sub>-NADP-ME grasses to deep shade reported a greater reduction in Rubisco activity in species from the open habitat (34%) relative to the shade habitat (3%). Likewise, NAD-ME species generally originate from relatively more open habitats than NADP-ME and PEP-CK species (Vogel *et al.*, 1986; Hattersley, 1992; Schulze *et al.*, 1996; Liu *et al.*, 2012). In addition, similar to the C<sub>3</sub> species, NAD-ME grasses may have a greater N flexibility by having higher leaf N relative to NADP-ME and PEP-CK counterparts.

Reduced Rubisco content is a common photosynthetic acclimation response to shade allowing optimal nitrogen allocation for maximal light harvesting (Boardman, 1977; Hikosaka and Terashima, 1995; Evans and Poorter, 2001; Walters, 2005). Consequently, lower Rubisco activity and activation may indicate a shift in photosynthetic limitation from Rubisco (sun leaves) to electron transport (shade leaves) (Evans, 1988; Evans and Poorter, 2001). Under shade, NAD-ME species had lower  $\Phi_{max}$  relative to NADP-ME and PEP-CK counterparts (Fig. 3). This difference may be

**Table 3.** Parameters derived from A–C, and light response curves for eight C<sub>4</sub> grasses grown under control (full sunlight) or shade (16% of natural sunlight) environments

Parameter	Treatment	Subtype			C <sub>4</sub>
		NADP-ME	PEP-CK	NAD-ME	
IS at HL ( $\mu\text{mol m}^{-2} \text{s}^{-1} \text{bar}^{-1}$ )	Control	0.5 ± 0.06 a	0.52 ± 0.02 a	0.62 ± 0.06 a	0.53 ± 0.03
	Shade	0.27 ± 0.03 a	0.27 ± 0.02 a	0.2 ± 0.02 a	0.25 ± 0.02
	% change	<b>−46</b>	<b>−49</b>	<b>−77</b>	<b>−54</b>
CSR at HL ( $\mu\text{mol m}^{-2} \text{s}^{-1}$ )	Control	42 ± 1 a	45 ± 1 a	41 ± 1 a	43 ± 1
	Shade	25 ± 1 b	23 ± 1 ab	15 ± 1 a	21 ± 1
	% change	<b>−39</b>	<b>−49</b>	<b>−64</b>	<b>−50</b>
IS/CSR at HL ( $\times 10^3$ )	Control	12 ± 1 a	12 ± 0 a	15 ± 1 a	12 ± 1
	Shade	10 ± 1 a	12 ± 1 a	13 ± 1 a	12 ± 1
	% change	−12	1	−9	−6
$A_{max}$ ( $\mu\text{mol m}^{-2} \text{s}^{-1}$ )	Control	53 ± 3 a	57 ± 1 a	58 ± 2 a	55 ± 1
	Shade	32 ± 2 a	26 ± 1 a	18 ± 3 a	28 ± 1
	% change	<b>−39</b>	<b>−54</b>	<b>−68</b>	<b>50</b>
Maximum quantum yield ( $\Phi_{max}$ ) ( $\text{mol mol}^{-1}$ )	Control	0.06 ± 0 a	0.07 ± 0 a	0.07 ± 0 a	0.07 ± 0
	Shade	0.05 ± 0 b	0.05 ± 0 b	0.03 ± 0 a	0.05 ± 0
	% change	<b>−19</b>	<b>−32</b>	<b>−55</b>	<b>−32</b>
Curvature ( $\theta$ ) of light response curve	Control	0.81 ± 0.04 b	0.57 ± 0.03 ab	0.53 ± 0.04 a	0.66 ± 0.03
	Shade	0.61 ± 0.04 a	0.64 ± 0.05 a	0.64 ± 0.05 a	0.62 ± 0.03
	% change	<b>−25</b>	12	19	−6

Values are means ±SE ( $n=3$ –4). The ranking (from lowest=a) of subtypes within each single row using multiple-comparison Tukey's post-hoc test. Values followed by the same letter are not significantly different at the 5% level. Significant fold changes are shown in bold ( $P<0.05$ ).

attributed to a greater inefficiency of the NAD-ME CCM, especially under shade as argued above. It could also be attributed to inherent inefficiencies of the light conversion apparatus in the NAD-ME subtype due to the burden of operating two fully fledged linear electron transport systems with granal chloroplasts in both MCs and BSCs. This is not the case for the NADP-ME subtype, and somewhat intermediate for the PEP-CK subtype (Ghannoum *et al.*, 2005, 2011). Taken together, these findings support our second hypothesis stating that larger photosynthetic reduction and acclimation in NAD-ME species is associated with their lower Rubisco activation and lower quantum efficiency relative to PEP-CK and NADP-ME species.

#### *Whole-plant implications of differential shade acclimation among the C<sub>4</sub> subtypes*

In the current study, CO<sub>2</sub> assimilation at growth light was equally reduced in NAD-ME (~81%), PEP-CK (~79%), and NADP-ME (~76%) species. However, total leaf area and plant DM were more profoundly reduced in NAD-ME (~92% and ~95%, respectively) than in PEP-CK (~81% and ~98%, respectively) and NADP-ME (~73% and ~81%, respectively) species. In addition to reduced leaf area, the larger reduction in plant DM for NAD-ME and PEP-CK species could also be attributed to reduced CCM efficiency and Φ<sub>max</sub>. Further, the  $R_d/A$  ratio increased to a greater extent in NAD-ME and PEP-CK (~3.5-fold) than in NADP-ME species (1.6-fold) under shade, which may result in a greater C loss in these two subtypes. Taken together, these findings suggest that shade may favour NADP-ME species due to their efficient CCM and quantum yield, and lower photosynthetic down-regulation and lower increase in  $R_d/A$  relative to NAD-ME and PEP-CK species.

This conclusion is supported by ecological observations. NAD-ME species are preferentially found in open and arid habitats relative to the other two C<sub>4</sub> subtypes (Osmond *et al.*, 1982; Vogel *et al.*, 1986; Hattersley, 1992; Schulze *et al.*, 1996; Liu *et al.*, 2012). On the one hand, most of the understorey C<sub>4</sub> grasses belong to the NADP-ME subtypes, such as *Setaria* species (Schulze *et al.*, 1996), *Paspalum* species (Ward and Woolhouse, 1986b; Klink and Joly, 1989; Firth *et al.*, 2002), and *Microstegium vimineum* (Barden, 1987). Moreover, NADP-ME species form dense canopy crops such as maize, Sorghum, Miscanthus, and sugarcane where most leaves are shaded (Sage, 2014).

It should be noted that a different light spectrum affects CCM efficiency in C<sub>4</sub> photosynthesis (Sun *et al.*, 2012). The light spectrum may vary in natural shade settings due to growth season, canopy compositions, and architecture (Ross *et al.*, 1986; Messier *et al.*, 1998). Therefore, an interaction effect between subtype and light spectral composition cannot be ignored, and further investigations are warranted.

#### *Conclusion*

Using C<sub>4</sub> grass from three biochemical subtypes and grown under full sunlight and shade (16% of full sunlight) conditions

equivalent to the light environment prevailing in lower crop canopies or forest understorey, this study demonstrated that NAD-ME and to a lesser extent PEP-CK species were generally outperformed by NADP-ME species under shade. This response was underpinned by a more efficient CCM and quantum yield in NADP-ME. These findings were corroborated by *in vivo* and *in vitro* measurements of C<sub>3</sub> and C<sub>4</sub> cycle enzymes, maximum quantum yield of PSII ( $\Phi_{max}$ ), photosynthetic carbon isotope discrimination ( $\Delta_p$ ), leaf dry matter δ<sup>13</sup>C, and total plant dry mass. Future research is needed to quantify the impact of respiration and photorespiration on carbon isotope discrimination ( $\Delta_p$ ) in the three biochemical subtypes of C<sub>4</sub> photosynthesis, as well as the significance of the secondary PEP-CK decarboxylase on photosynthetic responses to shade.

#### **Supplementary data**

Supplementary data are available at *JXB* online.

Table S1. Summary of plant growth parameters.

Table S2. Summary of gas exchange parameters.

Table S3. Summary of carbon isotope discrimination parameters.

Table S4. Summary of biochemical parameters.

Table S5. Definitions and units for variables described in the text.

Fig. S1. Glasshouse growth conditions.

Fig. S2. Photosynthetic CO<sub>2</sub> response curves ( $A-C_i$ ) of C<sub>4</sub> grasses.

Fig. S3. Photosynthetic light response curves for C<sub>4</sub> grasses.

Fig. S4. Sensitivity of leakiness at low light

Appendix S1. Leakiness calculations at low light

#### **Acknowledgments**

We thank Dr Craig Barton for support with the TDL measurements, and Mr Burhan Amiji for support with the setting up of the shade structure and data loggers. We also thank Fiona Koller for assistance in biochemical assays. BVS was supported by a postgraduate research award funded by the Australian Research Council and the Hawkesbury Institute for the Environment at Western Sydney University. This research was funded by the Australian Research Council: DP120101603 (OG and SMW), DE130101760 (RES), and CE140100015 (OG and SMW).

#### **References**

- Ashton AR, Burnell JN, Furbank RT, Jenkins CLD, Hatch MD.** 1990. Enzymes of C<sub>4</sub> photosynthesis. In: **Lea PJ**, ed. Methods in plant biochemistry. Volume 3. Enzymes in primary metabolism. London: Academic Press, 39–72.
- Barden LS.** 1987. Invasion of *Microstegium vimineum* (Poaceae), an exotic, annual, shade-tolerant, C<sub>4</sub> grass, into a North Carolina floodplain. American Midland Naturalist **118**, 40–45.
- Bates D, Maechler M, Bolker B, Walker S.** 2013. lme4: linear mixed-effects models using Eigen and S4. R Package Version 1.
- Bellasio C, Griffiths H.** 2014a. Acclimation of C<sub>4</sub> metabolism to low light in mature maize leaves could limit energetic losses during progressive shading in a crop canopy. Journal of Experimental Botany **65**, 3725–3736.
- Bellasio C, Griffiths H.** 2014b. Acclimation to low light by C<sub>4</sub> maize: implications for bundle sheath leakiness. Plant, Cell and Environment **37**, 1046–1058.

- Bellasio C, Griffiths H.** 2014c. The operation of two decarboxylases (NADP-ME and PEP-CK), transamination and partitioning of C<sub>4</sub> metabolic processes between mesophyll and bundle sheath cells allows light capture to be balanced for the maize C<sub>4</sub> pathway. *Plant Physiology* **164**, 466–480.
- Björkman O.** 1981. Responses to different quantum flux densities. In: **Lange OL, Nobel PS, Osmond CB, Ziegler H**, eds. *Physiological plant ecology I: responses to the physical environment*. Berlin, Heidelberg: Springer Berlin Heidelberg, 57–107.
- Björkman O, Holmgren P.** 1966. Photosynthetic adaptation to light intensity in plants native to shaded and exposed habitats. *Physiologia Plantarum* **19**, 854–859.
- Boardman NK.** 1977. Comparative photosynthesis of sun and shade plants. *Annual Review of Plant Physiology* **28**, 355–377.
- Bond WJ, Midgley GF.** 2012. Carbon dioxide and the uneasy interactions of trees and savannah grasses. *Philosophical Transactions of the Royal Society B: Biological Sciences* **367**, 601–612.
- Brown RH.** 1999. Agronomic implications of C<sub>4</sub> photosynthesis. In: **Sage RF, Monson RK**, eds. *C<sub>4</sub> plant biology*. San Diego: Academic Press, 473–507.
- Buchmann N, Brooks JR, Rapp KD, Ehleringer JR.** 1996. Carbon isotope composition of C<sub>4</sub> grasses is influenced by light and water supply. *Plant, Cell and Environment* **19**, 392–402.
- Cousins AB, Badger MR, von Caemmerer S.** 2008. C<sub>4</sub> photosynthetic isotope exchange in NAD-ME- and NADP-ME-type grasses. *Journal of Experimental Botany* **59**, 1695–1703.
- Edwards EJ, Osborne CP, Strömberg CA, et al.** 2010. The origins of C<sub>4</sub> grasslands: integrating evolutionary and ecosystem science. *Science* **328**, 587–591.
- Ehleringer J, Björkman O.** 1977. Quantum yields for CO<sub>2</sub> uptake in C<sub>3</sub> and C<sub>4</sub> plants: dependence on temperature, CO<sub>2</sub>, and O<sub>2</sub> concentration. *Plant Physiology* **59**, 86–90.
- Ehleringer JR, Cerling TE, Helliker BR.** 1997. C<sub>4</sub> photosynthesis, atmospheric CO<sub>2</sub>, and climate. *Oecologia* **112**, 285–299.
- Ehleringer J, Pearcy RW.** 1983. Variation in quantum yield for CO<sub>2</sub> uptake among C<sub>3</sub> and C<sub>4</sub> plants. *Plant Physiology* **73**, 555–559.
- Evans JR.** 1988. Acclimation by the thylakoid membranes to growth irradiance and the partitioning of nitrogen between soluble and thylakoid proteins. *Functional Plant Biology* **15**, 93–106.
- Evans JR, Poorter H.** 2001. Photosynthetic acclimation of plants to growth irradiance: the relative importance of specific leaf area and nitrogen partitioning in maximizing carbon gain. *Plant, Cell and Environment* **24**, 755–767.
- Evans JR, Sharkey TD, Berry JA, Farquhar GD.** 1986. Carbon isotope discrimination measured concurrently with gas exchange to investigate CO<sub>2</sub> diffusion in leaves of higher plants. *Functional Plant Biology* **13**, 281–292.
- Farquhar GD.** 1983. On the nature of carbon isotope discrimination in C<sub>4</sub> species. *Functional Plant Biology* **10**, 205–226.
- Farquhar GD, Cernusak LA.** 2012. Ternary effects on the gas exchange of isotopologues of carbon dioxide. *Plant, Cell and Environment* **35**, 1221–1231.
- Farquhar GD, Richards RA.** 1984. Isotopic composition of plant carbon correlates with water-use efficiency of wheat genotypes. *Functional Plant Biology* **11**, 539–552.
- Firth DJ, Jones RM, McFadyen LM, Cook BG, Whalley RDB.** 2002. Selection of pasture species for groundcover suited to shade in mature macadamia orchards in subtropical Australia. *Tropical Grasslands* **36**, 1–12.
- Furbank RT.** 2011. Evolution of the C<sub>4</sub> photosynthetic mechanism: are there really three C<sub>4</sub> acid decarboxylation types? *Journal of Experimental Botany* **62**, 3103–3108.
- Ghannoum O, Evans JR, Chow WS, Andrews TJ, Conroy JP, von Caemmerer S.** 2005. Faster Rubisco is the key to superior nitrogen-use efficiency in NADP-malic enzyme relative to NAD-malic enzyme C<sub>4</sub> grasses. *Plant Physiology* **137**, 638–650.
- Ghannoum O, Evans JR, von Caemmerer S.** 2011. Nitrogen and water use efficiency of C<sub>4</sub> plants. In: **Raghavendra AS, Sage RF**, eds. *C<sub>4</sub> photosynthesis and related CO<sub>2</sub> concentrating mechanisms*. Dordrecht: Springer Netherlands, 129–146.
- Gutierrez M, Gracen VE, Edwards GE.** 1974. Biochemical and cytological relationships in C<sub>4</sub> plants. *Planta* **119**, 279–300.
- Halekoh U, Højsgaard S.** 2014. A Kenward–Roger approximation and parametric bootstrap methods for tests in linear mixed models—the R package pbkrtest. *Journal of Statistical Software* **59**, 1–32.
- Hatch MD.** 1987. C<sub>4</sub> photosynthesis: a unique blend of modified biochemistry, anatomy and ultrastructure. *Biochimica et Biophysica Acta* **895**, 81–106.
- Hattersley PW.** 1982. δ<sup>13</sup> Values of C<sub>4</sub> types in grasses. *Functional Plant Biology* **9**, 139–154.
- Hattersley PW.** 1992. C<sub>4</sub> photosynthetic pathway variation in grasses (Poaceae): its significance for arid and semi-arid lands. In: **Chapman GP**, ed. *Desertified grasslands: their biology and management*. London: Academic Press, 181–212.
- Henderson SA, Caemmerer SV, Farquhar GD.** 1992. Short-term measurements of carbon isotope discrimination in several C<sub>4</sub> species. *Functional Plant Biology* **19**, 263–285.
- Hikosaka K, Terashima I.** 1995. A model of the acclimation of photosynthesis in the leaves of C<sub>3</sub> plants to sun and shade with respect to nitrogen use. *Plant, Cell and Environment* **18**, 605–618.
- Jenkins CL, Burnell JN, Hatch MD.** 1987. Form of inorganic carbon involved as a product and as an inhibitor of C<sub>4</sub> acid decarboxylases operating in C<sub>4</sub> photosynthesis. *Plant Physiology* **85**, 952–957.
- Kanai R, Edwards GE.** 1999. The biochemistry of C<sub>4</sub> photosynthesis. In: **Sage RF, Monson RK**, eds. *C<sub>4</sub> plant biology*. San Diego: Academic Press, 49–87.
- Klink CA, Joly CA.** 1989. Identification and distribution of C<sub>3</sub> and C<sub>4</sub> grasses in open and shaded habitats in São Paulo state, Brazil. *Biotropica* **21**, 30–34.
- Koteleva NK, Voznesenskaya EV, Edwards GE.** 2015. An assessment of the capacity for phosphoenolpyruvate carboxykinase to contribute to C<sub>4</sub> photosynthesis. *Plant Science* **235**, 70–80.
- Kromdijk J, Griffiths H, Schepers HE.** 2010. Can the progressive increase of C<sub>4</sub> bundle sheath leakiness at low PFD be explained by incomplete suppression of photorespiration? *Plant, Cell and Environment* **33**, 1935–1948.
- Kromdijk J, Schepers HE, Albanito F, Fitton N, Carroll F, Jones MB, Finn J, Lanigan GJ, Griffiths H.** 2008. Bundle sheath leakiness and light limitation during C<sub>4</sub> leaf and canopy CO<sub>2</sub> uptake. *Plant Physiology* **148**, 2144–2155.
- Kubásek J, Setík J, Dwyer S, Santrůček J.** 2007. Light and growth temperature alter carbon isotope discrimination and estimated bundle sheath leakiness in C<sub>4</sub> grasses and dicots. *Photosynthesis Research* **91**, 47–58.
- Leegood RC, Walker RP.** 2003. Regulation and roles of phosphoenolpyruvate carboxykinase in plants. *Archives of Biochemistry and Biophysics* **414**, 204–210.
- Liu H, Edwards EJ, Freckleton RP, Osborne CP.** 2012. Phylogenetic niche conservatism in C<sub>4</sub> grasses. *Oecologia* **170**, 835–845.
- Messier C, Parent S, Bergeron Y.** 1998. Effects of overstory and understory vegetation on the understory light environment in mixed boreal forests. *Journal of Vegetation Science* **9**, 511–520.
- Mook WG, Bommerson JC, Staverman WH.** 1974. Carbon isotope fractionation between dissolved bicarbonate and gaseous carbon dioxide. *Earth and Planetary Science Letters* **22**, 169–176.
- Ögren E, Evans JR.** 1993. Photosynthetic light-response curves. *Planta* **189**, 182–190.
- Ort DR, Merchant SS, Alric J, et al.** 2015. Redesigning photosynthesis to sustainably meet global food and bioenergy demand. *Proceedings of the National Academy of Sciences, USA* **112**, 8529–8536.
- Osmond CB, Winter K, Ziegler H.** 1982. Functional significance of different pathways of CO<sub>2</sub> fixation in photosynthesis. In: **Lange PDOL, Nobel PPS, Osmond PCB, Ziegler PDH**, eds. *Physiological plant ecology II*. Berlin: Springer Berlin Heidelberg, 479–547.
- Pearcy RW, Tumosa N, Williams K.** 1981. Relationships between growth, photosynthesis and competitive interactions for a C<sub>3</sub> and C<sub>4</sub> plant. *Oecologia* **48**, 371–376.
- Pengelly JJ, Sirault XR, Tazoe Y, Evans JR, Furbank RT, von Caemmerer S.** 2010. Growth of the C<sub>4</sub> dicot *Flaveria bidentis*:

- photosynthetic acclimation to low light through shifts in leaf anatomy and biochemistry. *Journal of Experimental Botany* **61**, 4109–4122.
- Pengelly JJ, Tan J, Furbank RT, von Caemmerer S.** 2012. Antisense reduction of NADP-malic enzyme in *Flaveria bidentis* reduces flow of CO<sub>2</sub> through the C<sub>4</sub> cycle. *Plant Physiology* **160**, 1070–1080.
- Pinto H.** 2015. Resource use efficiency of C<sub>4</sub> grasses with different evolutionary origins. PhD Thesis, University of Western Sydney, Australia.
- Pinto H, Sharwood RE, Tissue DT, Ghannoum O.** 2014. Photosynthesis of C<sub>3</sub>, C<sub>3</sub>-C<sub>4</sub>, and C<sub>4</sub> grasses at glacial CO<sub>2</sub>. *Journal of Experimental Botany* **65**, 3669–3681.
- Porra RJ, Thompson WA, Kriedemann PE.** 1989. Determination of accurate extinction coefficients and simultaneous equations for assaying chlorophylls a and b extracted with four different solvents: verification of the concentration of chlorophyll standards by atomic absorption spectroscopy. *Biochimica et Biophysica Acta* **975**, 384–394.
- R Core Team.** 2015. R: a language and environment for statistical computing. Vienna, Austria: R Foundation for Statistical Computing.
- Ross MS, Flanagan LB, Roi GHL.** 1986. Seasonal and successional changes in light quality and quantity in the understory of boreal forest ecosystems. *Canadian Journal of Botany* **64**, 2792–2799.
- Sage RF.** 2014. Stopping the leaks: new insights into C<sub>4</sub> photosynthesis at low light. *Plant, Cell and Environment* **37**, 1037–1041.
- Sage RF, McKown AD.** 2006. Is C<sub>4</sub> photosynthesis less phenotypically plastic than C<sub>3</sub> photosynthesis? *Journal of Experimental Botany* **57**, 303–317.
- Sage RF, Pearcy RW.** 2000. The physiological ecology of C<sub>4</sub> photosynthesis. In: **Leegood RC, Sharkey TD, Caemmerer SV**, eds. Photosynthesis. Dordrecht: Springer Netherlands, 497–532.
- Saintilan N, Rogers K.** 2015. Woody plant encroachment of grasslands: a comparison of terrestrial and wetland settings. *New Phytologist* **205**, 1062–1070.
- Schulze ED, Ellis R, Schulze W, Trimborn P, Ziegler H.** 1996. Diversity, metabolic types and δ<sup>13</sup>C carbon isotope ratios in the grass flora of Namibia in relation to growth form, precipitation and habitat conditions. *Oecologia* **106**, 352–369.
- Sharwood RE, Ghannoum O, Kapralov MV, Gunn LH, Whitney SM.** 2016a. Temperature responses of Rubisco from Paniceae grasses provide opportunities for improving C<sub>3</sub> photosynthesis. *Nature Plants* **2**, 16186.
- Sharwood RE, Sonawane BV, Ghannoum O.** 2014. Photosynthetic flexibility in maize exposed to salinity and shade. *Journal of Experimental Botany* **65**, 3715–3724.
- Sharwood RE, Sonawane BV, Ghannoum O, Whitney SM.** 2016b. Improved analysis of C<sub>4</sub> and C<sub>3</sub> photosynthesis via refined *in vitro* assays of their carbon fixation biochemistry. *Journal of Experimental Botany* **67**, 3137–3148.
- Sharwood RE, von Caemmerer S, Maliga P, Whitney SM.** 2008. The catalytic properties of hybrid Rubisco comprising tobacco small and sunflower large subunits mirror the kinetically equivalent source Rubiscos and can support tobacco growth. *Plant Physiology* **146**, 83–96.
- Stutz SS, Edwards GE, Cousins AB.** 2014. Single-cell C<sub>4</sub> photosynthesis: efficiency and acclimation of *Biennertia sinuspersici* to growth under low light. *New Phytologist* **202**, 220–232.
- Sugiyama T, Mizuno M, Hayashi M.** 1984. Partitioning of nitrogen among ribulose-1,5-bisphosphate carboxylase/oxygenase, phosphoenolpyruvate carboxylase, and pyruvate orthophosphate dikinase as related to biomass productivity in maize seedlings. *Plant Physiology* **75**, 665–669.
- Sun W, Ubierna N, Ma JY, Cousins AB.** 2012. The influence of light quality on C<sub>4</sub> photosynthesis under steady-state conditions in *Zea mays* and *Miscanthus × giganteus*: changes in rates of photosynthesis but not the efficiency of the CO<sub>2</sub> concentrating mechanism. *Plant, Cell and Environment* **35**, 982–993.
- Tazoe Y, Hanba YT, Furumoto T, Noguchi K, Terashima I.** 2008. Relationships between quantum yield for CO<sub>2</sub> assimilation, activity of key enzymes and CO<sub>2</sub> leakiness in *Amaranthus cruentus*, a C<sub>4</sub> dicot, grown in high or low light. *Plant and Cell Physiology* **49**, 19–29.
- Tazoe Y, Noguchi K, Terashima I.** 2006. Effects of growth light and nitrogen nutrition on the organization of the photosynthetic apparatus in leaves of a C<sub>4</sub> plant, *Amaranthus cruentus*. *Plant, Cell and Environment* **29**, 691–700.
- Ubierna N, Gandin A, Boyd RA, Cousins AB.** 2017. Temperature response of mesophyll conductance in three C<sub>4</sub> species calculated with two methods: 18O discrimination and *in vitro* V<sub>pmax</sub>. *New Phytologist* **214**, 66–80.
- Ubierna N, Sun W, Kramer DM, Cousins AB.** 2013. The efficiency of C<sub>4</sub> photosynthesis under low light conditions in *Zea mays*, *Miscanthus × giganteus* and *Flaveria bidentis*. *Plant, Cell and Environment* **36**, 365–381.
- Vogel JC, Fuls A, Danin A.** 1986. Geographical and environmental distribution of C<sub>3</sub> and C<sub>4</sub> grasses in the Sinai, Negev, and Judean deserts. *Oecologia* **70**, 258–265.
- von Caemmerer S.** 2000. Biochemical models of leaf photosynthesis. Collingwood, Australia: CSIRO Publishing.
- von Caemmerer S, Farquhar GD.** 1981. Some relationships between the biochemistry of photosynthesis and the gas exchange of leaves. *Planta* **153**, 376–387.
- von Caemmerer S, Ghannoum O, Pengelly JJ, Cousins AB.** 2014. Carbon isotope discrimination as a tool to explore C<sub>4</sub> photosynthesis. *Journal of Experimental Botany* **65**, 3459–3470.
- Walters RG.** 2005. Towards an understanding of photosynthetic acclimation. *Journal of Experimental Botany* **56**, 435–447.
- Wang Y, Bräutigam A, Weber AP, Zhu XG.** 2014. Three distinct biochemical subtypes of C<sub>4</sub> photosynthesis? A modelling analysis. *Journal of Experimental Botany* **65**, 3567–3578.
- Ward DA, Woolhouse HW.** 1986a. Comparative effects of light during growth on the photosynthetic properties of NADP-ME type C<sub>4</sub> grasses from open and shaded habitats. I. Gas exchange, leaf anatomy and ultrastructure. *Plant, Cell and Environment* **9**, 261–270.
- Ward DA, Woolhouse HW.** 1986b. Comparative effects of light during growth on the photosynthetic properties of NADP-ME type C<sub>4</sub> grasses from open and shaded habitats. II. Photosynthetic enzyme activities and metabolism. *Plant, Cell and Environment* **9**, 271–277.
- Winter K, Schmitt MR, Edwards GE.** 1982. *Microstegium vimineum*, a shade adapted C<sub>4</sub> grass. *Plant Science Letters* **24**, 311–318.
- Zhu XG, Long SP, Ort DR.** 2008. What is the maximum efficiency with which photosynthesis can convert solar energy into biomass? *Current Opinion in Biotechnology* **19**, 153–159.